Synthesis and Characterization of Soluble Poly(ferrocenylenearylene)s from Condensation of Dilithio Bis(alkylcyclopentadienide)arenes with Iron(II) Halides: A General Route to Conjugated Poly(metallocene)s

Glen E. Southard and M. David Curtis*

Department of Chemistry, Willard H. Dow Laboratory, The University of Michigan, Ann Arbor, Michigan 48109-1055

Received August 18, 2000

Bis(alkylcyclopentadienyl)arenes have been prepared by sequential lithiation/alkylation of dibromoarenes with alkylcyclopenta-2-en-1-ones. The resulting dicarbinols were dehydrated with *p*-toluenesulfonic acid to give the bis(alkylcyclopentadienyl)arene. Poly(alkyl-1,1′-ferrocenylenearylene)s were prepared by the reaction of dilithio bis(alkylcyclopentadienide)-arenes and iron(II) salts in THF. The resulting polymers were oxidized with iodine to give the fully oxidized polyionomers. The polyionomers were found to give mixed-valence polymers when allowed to equilibrate with neutral polymers in solution, provided the degree of oxidation, N, lies between ca. 0.55 and 1.0. For degrees of oxidation $0.0 < N < 0.55$, disproportionation occurs to give neutral polymer and polymer with $N \approx 0.55$. The oxidized polymers showed small to moderate antiferromagnetic interactions, and some were found to follow non-Curie−Weiss behavior that is ascribed to the complex magnetic properties of individual ferrocenium centers rather than to any type of magnetic ordering. The organic bridging ligands and polymers were characterized by TGA-DSC, GPC, NMR, CV, FT-IR, and UV−vis techniques. The fully oxidized and mixed-valence polymers were characterized by magnetic susceptibility, FT-IR, EPR, Mössbauer, and UV−vis spectroscopies.

Introduction

Conjugated organometallic polymers have received much attention for their electroactive and magnetic properties for use in applications, e.g., NLO devices,[1] light emitting diodes (LEDs),[2] electrochromic thin films,[3] macrocyclic precursors,[4] and thin film transistors (TFTs).[5] The combination of the electroactivity of transition metals with the electronic properties of conjugated polymers is an attractive strategy for enhancing the physical and electronic properties of the resultant hybrid polymers.[6] Electronic delocalization along the polymeric chain may also enhance the communication between metal centers, thus allowing the magnetic and spectroscopic properties to be fine-tuned for specific applications, while the extent of delocalization is influenced by the nature of the bridging ligands. Ferrocene was chosen for initial study as the redox active building block, in view of its wide use in organometallic chemistry, its having two stable oxidation states, its thermal stability, and its ease of preparation.

Polyferrocenes have been synthesized via a number of routes: thermal, nucleophilic, and transition-metal-catalyzed ring-opening polymerization,[7] atom abstraction polymerization,[8] Heck coupling polymerization,[9]

(1) (a) Wright, M. E.; Toplikan, E. G. *Macromolecules* **1992**, *25*, 6050. (b) Yuan, Z.; Stringer, G.; Jobe, I. R.; Kreller, D.; Scott, K.; Koch, L.; Taylor, N.; Marder, T. B. *J. Organomet. Chem.* **1993**, *452*, 115. (c) Myers, L. K.; Langhoff, C.; Thompson, M. E. *J. Am. Chem. Soc.* **1992**, *114*, 7560.

(2) (a) Bradley, D. D. C. *Synth. Met.* **1993**, *54*, 401. (b) Inganäs, O.; Berggren, M.; Andersson, M. R.; Gustafsson, G.; Hjertberg, T.; Wennerström, O.; Dyreklev, P.; Granström, M. *Synth. Met.* **1995**, *71*, 2121. (c) Greiner, A.: Bolle, B.; Hesemann, P.; Oberski, J. M.; Sander, R. *Macromol. Chem. Phys.* **1996**, *197*, 113.

(3) Nguyen, M. T.; Diaz, A. F.; Dement'ev, V. V.; Pannell, K. H. *Chem. Mater.* **1994**, *6*, 952.

(4) (a) Barlow, S.; O'Hare, D. *Organometallics* **1996**, *15*, 3885. (b) Altmann, M,; Friedrich, J. Beer, F. Reuter, R.; Enkelmann, V.; Bunz, U. H. F. *J. Am. Chem. Soc.* **1997**, *119*, 1472. (c) Mueller-Westerhoff, U. T. *Angew. Chem., Int. Ed. Engl.* **1986**, *25*, 702.

(5) Dodabalapur, A.; Torsi, L.; Katz, H. E. *Science* **1995**, *268*, 270.

(6) (a) Pudelski, J. K.; Foucher, D. A.; Honeyman, C. H.; Macdonald, P. M.; Manners, I.; Barlow, S.; O'Hare, D. *Macromolecules* **1996**, *29*, 1894. (b) Bund, E. E.; Campos, P.; Ruz, J.; Valle, L.; Chadwick, I.; Santa Ana, M.; Gonzalez, G.; Manriquez, J. M. *Organometallics* **1988**, *7*, 474. (c) Meng, X., Sabat, M., Grimes, R. N. *J. Am. Chem. Soc.* **1993**, *115*, 6143. (d) Bunel, E. E.; Valle, L.; Carroll, P. J.; Gonzalez, M.; Munoz, N.; Manriquez, *J. M. Organometallics* **1988**, *7*, 789. (e) Rosenblum, M.; Nugent, H. M.; Jang, K. S.; Labes, M. M.; Cahalane, W.; Klemarczyk, P.; Reiff, W. M. *Macromolecules* **1995**, *28*, 6330. (f) Hirao, T.; Kurashina, M.; Aramaki, K.; Nishihara, H. *J. Chem. Soc., Dalton Trans.* **1996**, 2929. (g) Altmann, M.; Friedrich, J.; Beer, F.; Reuter, R.; Enkelmann, V.; Bunz, U. H. F. *J. Am. Chem. Soc.* **1997**, *119*, 1472 (h) Southard, G. E.; Curtis, M. D. *Organometallics* **1997**, *16*, 5618.

(7) (a) Manners, I. *Adv. Organomet. Chem.* **1995**, *37*, 131. (b) Rulkens, R.; Lough, A. J.; Manners, I. *J. Am. Chem. Soc.* **1994**, *116*, 797 (c) Reddy, N. P.; Yamashita, H.; Tanaka, M. *J. Chem. Soc., Chem. Commun.* **1995**, 2263. (d) MacLachlan M. J.; Zheng, J.; Lough, A. J.; Manners, I.; Mordas, C.; LeSuer, R.; Geiger, W. E.; Liable-Sands, L. M.; Rheingold, A. L. *Organometallics* **1999**, *18*, 1337.

(8) (a) Compton, D. L.; Brandt, P. F.; Rauchfuss, T. B.; Rosenbaum, D. F.; Zukoski, C. F. *Chem. Mater.* **1995**, *7*, 2342 (b) Compton, D. L.; Rauchfuss, T. B. *Organometallics* **1994**, *13*, 4367.

(9) Bochmann, M.; Lu, J.; Cannon, R. D. J. *Organomet. Chem.* **1996**, *518*, 97.

10.1021/om000722z CCC: $20.00
Publication on Web 12/20/2000

polycondensation of lithiated bisfulvene and ferrous halide,[10] transition-metal-catalyzed coupling of dihaloarenes and diethynylarenes,[11] acyclic diene metathesis polymerization,[12] Knoevenagel condensation polymerization,[13] and Suzuki coupling polymerization.[14] Two excellent reviews have summarized recent developments in the synthesis and materials properties of metal-containing polymers.[15]

Since Cowan and co-workers reported electron transfer in the monocation of biferrocene,[16] a great number of binuclear ferrocene derivatives have been prepared and studied.[17−20] However, while a number of polymers containing ferrocene moieties have been prepared, few have had their mixed-valence properties investigated. The possibility of strong magnetic coupling of metal centers mediated by conjugated linking groups is especially intriguing. Manriquez et al. found that the magnetic susceptibility of (Cp_2Fe)(s-indacene)$^{+2}$ could not be described by a single Curie−Weiss (CW) expression and took this as evidence for magnetic ordering.[20d] Garnier et al. interpreted similar data to indicate ferromagnetic coupling in a partially oxidized oligo(ferrocenylenedialkylsilylene),[16] a claim that Manners and co-workers could not substantiate.[6a]

As can be seen from the above discussion, the presence or absence of magnetic ordering of the paramagnetic iron centers in partially or fully oxidized ferrocene oligomers or polymers is unsettled. The magnetic behavior of ferrocenium ions is complicated by its electronic ground state, $^2E_{2g}$, and a low lying excited state, $^2A_{1g}$, whose population is influenced by the electron-donating ability of the Cp substituents, the symmetry of the ferrocenium environment, and the temperature.[21] The relative populations of the ground and first excited state influence the magnetic moment and the shape of χ^{-1} vs temperature plots. Hence, the non-CW behavior of the some of the reported systems might be attributable to the electronic structure of the ferrocenium cation itself, rather than to long-range magnetic interactions or ordering phenomena. However, problems with determining the degree of oxidation of insoluble polymers, decomposition of the oxidizing agent, and the possible presence of trace paramagnetic impurities have made progress difficult. The goals of the present research were to develop a general methodology for the preparation of conjugated metallocene polymers, to synthesize soluble, readily characterized, conjugated poly(ferrocene)s as a test case, and to study their electronic and magnetic properties vs the degree of oxidation in order to illuminate the nature of the electronic and magnetic interactions between metal centers.

Chart 1

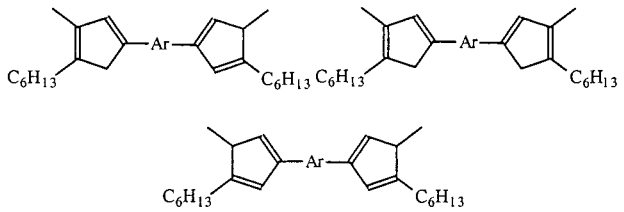

Results and Discussion

Monomer Synthesis. We have found that conjugated poly(ferrocenylenearylene)s tend to be sparsely soluble unless the polymer backbone is substituted with pendant, long-chain alkyl groups. Asymmetric substitution also enhances solubility. Thus, we have developed a route to alkylated bis(cyclopentadienyl)arene "monomers" that are useful for the preparation of soluble metallocene polymers. The route is an adaptation of the synthesis of bis(tetramethylcyclopentadienyl)benzene.[22] The monomer precursor, 3-hexyl-4-methylcyclopent-2-en-1-one,[23] was prepared by the condensation of 2-nonenoic acid and 2-propanol with a catalytic amount of sulfuric acid to give isopropyl-2-nonenoate in 95% yield.[24] The ester was then converted to 3-hexyl-4-methylcyclopent-2-en-1-one by the reaction of the ester with polyphosphoric acid (PPA) at 100 °C for 12 h.[24] The cyclopentadienone was then converted to the desired bis(cyclopentadienyl)arene ligands by monolithiation of 1,4-dibromobenzene or 2,5-dibromothiophene with 1 equiv of *n*-butyllithium in diethyl ether, reaction of the lithio reagent with the ketone, followed by a repetition of the lithiation and a second equivalent of 3-hexyl-4-methylcyclopent-2-en-1-one. This series of reactions gives the diols, which were converted to the alkylated bis(cyclopentendienyl)arene monomers upon subsequent dehydration with *p*-toluenesulfonic acid in 21−52% yield (Scheme 1).[24]

The 1,4-bis(3-hexyl-4-methylcyclopentadienyl)benzene may be recrystallized from hexanes as a light yellow solid. As determined by ^{1}H NMR, the solid consists of three isomers, tentatively assigned to those shown in Chart 1. The 2,5-bis(3-hexyl-4-methylcyclopentadienyl)-thiophene is a liquid down to −40 °C, but may be purified by flash chromatography over silica gel with hexanes as eluent. ^{1}H NMR assignments of 2,5-bis(3-

(10) Hirao, T.; Kurashina, M.; Aramake, K.; Nishihara, H. *J. Chem. Soc., Dalton Trans.* **1996**, 2929.
(11) (a) Yamamoto, T.; Morikita, T.; Maruyama, T.; Kubota, K.; Katada, M. *Macromolecules* **1997**, *30*, 5390. (b) Morikita, T.; Maruyama, T.; Yamamoto, T.; Kubota, K.; Katada, M. *Inorg. Chim. Acta* **1998**, *269*, 310.
(12) (a) Tilley, T. D.; Buretea, M. A. *Organometallics* **1997**, *16*, 1507. (b) Gamble, A. S.; Patton, J. T.; Boncella, J. M. *Makromol. Chem., Rapid Commun.* **1992**, *13*, 109−115. (c) Heo, R. W.; Somoza, F. B.; Lee, T. R *J. Am. Chem. Soc.* **1998**, *120*, 1621.
(13) Wright, M. E.; Sigman, M. S. *Macromolecules* **1992**, *25*, 6055.
(14) Knapp, R.; Velten, U.; Rehahn, M. *Polymer* **1998**, *39(23)*, 5827.
(15) (a) Nguyen, P.; Gomez-Elipe, P.; Manners, I. *Chem. Rev.* **1999**, *99*, 1515. (b) Kingsborough, R. P.; Swager, T. M. *Prog. Inorg. Chem.* **1999**, *48*, 123.
(16) Levanda, C.; Cowan, D. O.; Leitch, C.; Bechgaard, K. *J. Am. Chem. Soc.* **1974**, *96*, 6788.
(17) Hyene, M.; Yassar, A.; Escorne, M.; Percheron-Guegan, A.; Garnier, F. *Adv. Mater.* **1994**, *6*, 564.
(18) Posselt, D.; Badur, W.; Steiner, M. *Synth. Met.* **1993**, *55−57*, 3299.
(19) (a) Thomas, K. R. J.; Lin, J. T.; Wen, Y. S. *Organometallics* **1999**, *19*, 1008. (b) Deck, P. A.; Lane, M. J.; Montgomery, J. L.; Slebodnick, C.; Fronczek, F. R. *Organometallics* **1999**, *19*, 1013. (c) Le Stang, S.; Paul, F.; Lapinte, C. *Organometallics* **1999**, *19*, 1035. (d) Barlow, S.; Marder, S. R. *Chem. Commun.* **2000**, 1555.
(20) (a) Morrison, W. H., Jr.; Hendrickson, D. N. *Inorg. Chem.* **1975**, *14*, 2331. (b) Morrison, W. H., Jr.; Krogsrud, S.; Hendrickson, D. N. *Inorg. Chem.* **1973**, *12*, 1998. (c) Morrison, W. H., Jr.; Hendrickson, D. N. *Inorg. Chem.* **1974**, *13*, 2279. (d) Manriquez, J. M.; Ward, M. D.; Reiff, W. M.; Calabrese, J. C.; Jones, N. L.; Carroll, P. J.; Bunel, E. E.; Miller, J. S. *J. Am. Chem. Soc.* **1995**, *117*, 6182.
(21) Hendrickson, D. N.; Sohn, Y. S.; Gray, H. B. *Inorg. Chem.* **1971**, *10*, 1559.
(22) Kohl, F. X.; Jutzi, P. *J. Organomet. Chem.* **1983**, 119.
(23) (a) Meng, X., Sabat, M., Grimes, R. N. *J. Am. Chem. Soc.* **1993**, *115*, 6143. (b) Bund, E. E.; Campos, P.; Ruz, J.; Valle, L.; Chadwick, I.; Santa Ana, M.; Gonzalez, G.; Manriquez, J. M. *Organometallics* **1988**, *7*, 474, (c) Conia, J. M.; Leriverand, M. L. *Bull. Soc. Chim. Fr.* **1970**, 2981.
(24) Tiollais, P. *Bull. Soc. Chim. Fr.* **1947**, 708.

Scheme 1

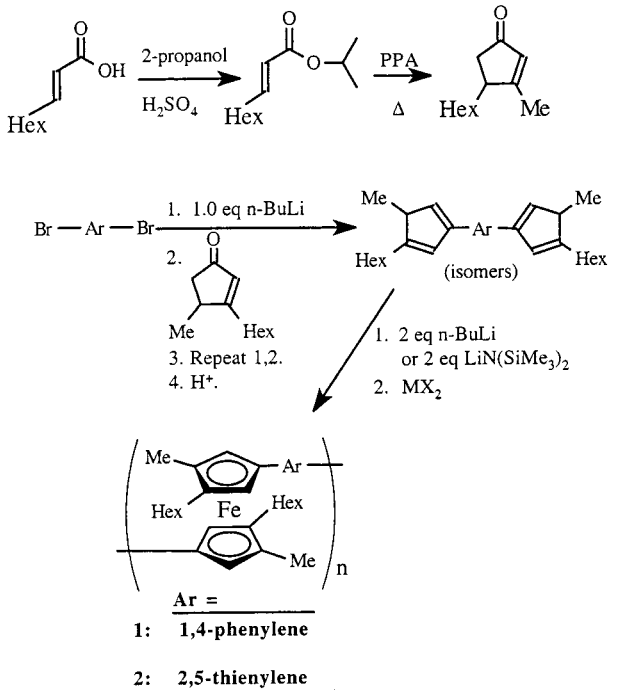

hexyl-4-methylcyclopentadienyl)thiophene are complicated by the presence of many of the 25 possible isomers corresponding to the various positions of the double bonds in the Cp rings.

Polymer Synthesis. The ligands, 1,4-bis(3-hexyl-4-methylcyclopentadienyl)benzene and 2,5-bis(3-hexyl-4-methylcyclopentadienyl)thiophene, were converted to their respective dilithio salts with 2 equiv of lithium bis(trimethylsilyl)amide in THF.[25] The dilithium salts were allowed to react with an equimolar amount of ferrous iodide in THF. The reaction mixture was heated to reflux for at least 4 days before being precipitated by adding the mixture to methanol. Dilithium 1,4-bis(3-hexyl-4-methylcyclopentadienide)benzene precipitated from THF solution, resulting in a stoichiometric imbalance if an equimolar amount of anhydrous FeI_2 was added all at once (method A). The nonstoichiometry results in the formation of a large amount of cyclic dimers, trimers, and higher, cyclic oligomers. However, if small increments of anhydrous FeI_2 were added over the interval of several days (method B), then the cyclization problem was lessened. Poly(3,3′-dihexyl-4,4′-dimethyl-1,1′-ferrocenylene-*alt*-1,4-phenylene) (**1**) and poly(3,3′-dihexyl-4,4′-dimethyl-1,1′-ferrocenylene-*alt*-2,5-thienylene) (**2**) were collected in 71 and 50% yields, respectively.

Polymer Characterization. Microanalysis of the aforementioned polymers gave good agreement between theoretical and experimental results for the expected repeat unit, as shown in the Scheme 1. Polymer **1** prepared by method B had a C,H-analysis that indicated the presence of end-groups (nonmetalated Cp-rings) with a number average degree of polymerization of ca. 7, a value in good agreement with the results of GPC analysis (see below). However, elemental percentages for infinite polymer and cyclic oligomers are identical; hence, microanalysis alone is not suitable for establishing the degree of polymerization. Fast atom bombardment mass spectroscopy (FABS) of **1** revealed peaks at 912, 1368, and 1825 *m*/*z*, which correspond well with the molecular weight of cyclic dimer (912 g/mol), trimer (1368 g/mol), and tetramer (1824 g/mol). Indeed, the cyclic dimer (**3**, Chart 2) could be isolated by high-temperature sublimation from **1**. No masses associated with noncyclic oligomers were observed. GPC traces of the soluble polymers **1** and **2** also revealed the presence of significant amounts of cyclic oligomers as well as polymer. A GPC (calibrated vs polystyrene standards) trace of **2** had two distinguishable peaks in the low molecular weight region corresponding to masses of 950 and 1644 g/mol, in good agreement with the molecular weights of the cyclic dimer (924) and trimer (1386). Thus, the rate of cyclization is competitive with the rate of polymerization under reaction conditions, and the presence of cyclic oligomers results in a low M_n and a very broad PDI, as seen in Table 1. All the characterizations described below were performed on the samples with the characteristics reported in Table 1.

Table 1. Molecular Weight Data for Poly(1,1′-ferrocenylenearylenes)s[a]

polymer	yield (%)	M_n	M_w	PDI	DP[b]
1	71	4×10^3	4.2×10^4	10.5	8.8
2	50	3.6×10^3	5.3×10^4	14.6	7.8

[a] Determined by GPC, chloroform solvent, polystyrene standards, 1 mL/min flow rate, UV detector. [b] Degree of polymerization.

Chart 2

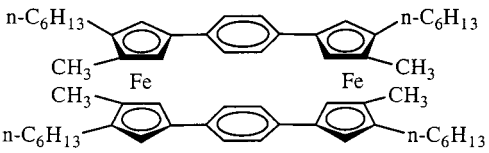

Thermal Analysis. Thermogravimetric analysis (TGA, heating rate of 40 °C/min, N_2 atmosphere) of **1** and **2** revealed a high thermal stability of these materials with decomposition temperatures (indicated by 5% mass loss) of 406 and 440 °C, respectively. The char yields of **1** and **2** are 28% and 25% at 900 °C, respectively. Once decomposition began, mass loss was steady with no distinguishing features. High-temperature decomposition of **1** in a mass spectrometer produced fragments with $m/z = 58$ and 114, indicating loss of butane and octane. The primary decomposition of **1** appears to be loss of butyl radicals followed by H-atom abstraction or coupling. Differential scanning calorimetry (DSC, heating rate of 20 °C/min, under N_2) of **1** revealed a weak melting endotherm ($T_m = 72$ °C, $\Delta H = 4.8$ J/g), but no T_g was observed. On the other hand, polymer **2** was observed to have a weak glass transition ($T_g = 30$ °C, $\Delta Cp = 0.32$ J/g °C), but no T_m was observed. Low melting temperatures are expected for polymers with large alkyl pendant groups, and glass transitions are often not observed for similar polymers.[26]

(25) Rosenblum, M.; Nugent, H. M.; Jang, K. S.; Labes, M. M.; Cahalane, W.; Klemarczyk, P.; Reiff, W. M. *Macromolecules* **1995**, *28*, 6330.

(26) (a) Foucher, D. A.; Ziembinski, R.; Tang, B.; Macdonald, P. M.; Massey, J.; Jaeger, C. R.; Jaeger, Vancso, G. J.; Manners, I. *Macromolecules* **1993**, *26*, 2878. (b) Foucher, D. A.; Ziembinski, R.; Peterson, R.; Pudelski, J.; Edwards, M.; Ni, Y.; Macdonald, P. M.; Massey, J.; Jaeger, C. R. Jaeger, Vansco, G. J.; Manners, I. *Macromolecules* **1994**, *27*, 3992.

Chart 3

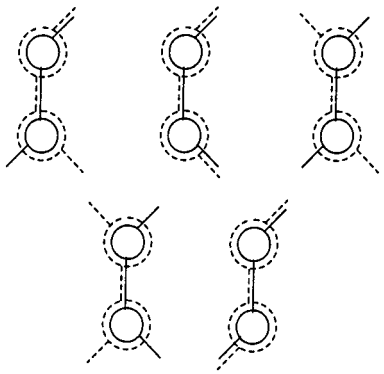

Nuclear Magnetic Resonance. ^{1}H NMR spectra of solutions of **1** and **2** exhibited broad signals due to geometrical isomerism of the pendant alkyl groups. Dimer **3** has five possible geometric isomers, two of which are chiral, as seen in Chart 3. Hence, the mixture of geometrical isomers and the distribution of cyclic oligomers and polymers give rise to broad signals in the ^{1}H NMR spectra.

Surprisingly, ^{13}C NMR spectra of the polymers exhibited fairly narrow signals that revealed little evidence of isomerism. For example, the spectrum of **1** had two narrow signals at 136.0 and 122.2 ppm, which were assigned to the carbon atoms of the bridging phenylene group, and five narrow and distinct signals at 89.5, 84.5, 83.9, 69.4, and 68.4 ppm, assignable to cyclopentadienyl carbons.

UV−Vis. UV−vis spectroscopy of ferrocene and its derivatives has been studied extensively. So-called band II of ferrocene ($\lambda_{max} \approx 440$ nm, $\epsilon = 100$ M^{-1} cm^{-1}, assigned to a spin allowed d−d transition) is useful in characterizing ferrocene derivatives because it is relatively strong and well resolved from other absorptions.[27] UV−vis spectra of **1**, **2**, and the cyclic dimer, **3**, exhibited band II absorptions at 460 nm ($\epsilon = 2000$ M^{-1} cm^{-1}), 468 nm ($\epsilon = 2800$ M^{-1} cm^{-1}), and 455 nm ($\epsilon = 870$ M^{-1} cm^{-1}), respectively. The molar extinction coefficients of all polymers are reported as per mole of metal and are considerably larger than those of simple ferrocenes ($\epsilon = 100-200$ M^{-1} cm^{-1}). The large difference between the molar absorptivities of **1** and **3** may be attributed to their geometries. Rigid biferrocenes analogous to **3** also have low molar absorptivities ($\epsilon = 255-650$ M^{-1} cm^{-1}).[28,29] Spangler and co-workers have studied the electronic spectra of a series of α,ω-diferrocenylpolyenes of the general formula $F_c-(CH{=}CH)_n-F_c$, where $n = 1-6$. The molar extinction coefficients of both the vinylene bridge $\pi \rightarrow \pi^*$ and Fc band II absorptions increased as the length of the vinylene bridge increased. Thus, the ferrocene group is not an independent chromophore, and there is significant ligand π^* character in the "d−d" transition.[30,31]

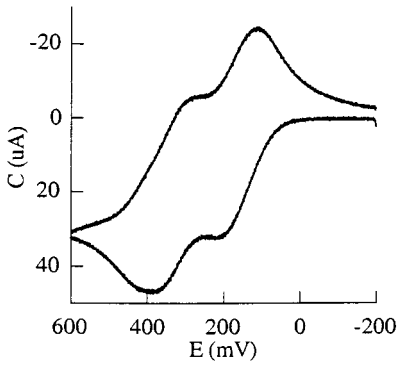

Figure 1. Cyclic voltammogram of **1**. Data obtained at 23 °C in CH_2Cl_2 solution of 0.1 M NBu_4PF_6 electrolyte at a scan rate of 100 mV/s.

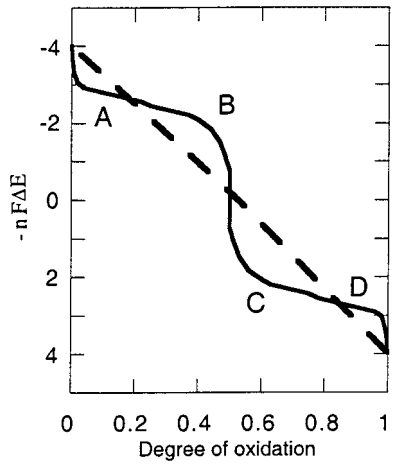

Figure 2. Potential vs degree of oxidation for conjugated polymetallocenes (adapted from ref 32).

Electrochemistry. Cyclic voltammetry of **1** and **2** in methylene chloride solution with 0.1 M Bu_4NPF_6 electrolyte showed moderate electronic interaction between metal centers, as indicated by the presence of two reversible waves of equal intensity (cf. Figure 1). For **1**, a plot of current vs the square root of scan rate was linear over the range of scan rates employed, indicative of diffusion-controlled electron transfer. The first wave ($E = {}^1E_{1/2}$ at −0.24 and −0.20 V for **1** and **2**, respectively) is followed by a second wave at higher potential ($E = {}^2E_{1/2}$ at −0.07 (**1**) and −0.01 V (**2**)). These waves have been attributed to the oxidation of alternate metal centers along the polymer backbone at the first wave and oxidation of the remaining metal centers at the second. However, the situation is not that simple. Aoki and Chen have analyzed the oxidation of polynuclear, linear complexes of redox active centers by the correlated-walk technique.[32] Their results may be presented as a Frost diagram,[33] a plot of $-nF\Delta E°$ (= the free energy) vs the degree of oxidation (N) of the polymer, as shown in Figure 2 (adapted from Figure 7 of ref 32). As Figure 2 shows, the oxidation potential shows an initially sharp increase as the polymer is oxidized, but then the potential plateaus up to about $N = 0.45$. Then a very large increase in potential occurs in the range $0.45 < N < 0.55$, followed by another plateau and a final, small increase. With

(27) Sohn, Y. S.; Hendrickson, D. N.; Gray, B. G. *J. Am. Chem. Soc.* **1971**, *93*, 3603.
(28) Hedberg, F. L.; Rosenberg, H. *J. Am. Chem. Soc.* **1969**, *91*, 1258.
(29) Kaufman, F.; Cowan, D. O., H. *J. Am. Chem. Soc.* **1970**, *92*, 6198.
(30) (a) Toma, S.; Gaplovsky, A.; Hudecek, M.; Langfelderova, Z. *Monatsh. Chem.* **1985**, *116*, 357 (b) Toma, S.; Gaplovsky, A.; Elecko, P. *Chem. Pap.* **1985**, *39*, 115.
(31) Ribou, A.; Launay, J.; Sachtleben, M. L.; Li, J.; Spangler, C. W. *Inorg. Chem.* **1996**, *35*, 3735.
(32) Aoki, K.; Chen, J. *J. Electroanal. Chem.* **1995**, *380*, 35.
(33) Frost, A. A. *J. Am. Chem. Soc.* **1951**, *73*, 2680.

Table 2. Comparison of ΔE vs Iron−Iron Distances

entry no.	compound	$^1E_{1/2}$, V	$^2E_{1/2}$, V	ΔE,[a] V	d_{Fe},[b] Å	K_c
1	$[C_2H_2(C_{10}H_8Fe)]_n$[12a]			0.250	7.03	1.7×10^4
2	$[(C_4H_4(C_{10}H_9Fe)_2]$[31]			0.129	9.21	150
3	$[S_2(C_4H_9C_5H_4)(C_5H_4)Fe]_n$[8b]			0.290	8.62	7.8×10^4
4	$[C_2H_4(C_{10}H_8Fe)]_n$[52]			0.090	7.70	33
5	$[SiMe_2(C_{10}H_8Fe)]_n$[53]			0.250	6.30	1.7×10^4
6	$C_6H_4[(C_2C_5H_4)_2Fe]_n$[9]			0.0	13.7	1.0
7	**1**	−0.24	−0.07	0.170	9.0	750
8	**2**	−0.20	−0.01	0.190	8.6	1630
9	**PDCP-Br-100**[c]	−1.59	−1.37	0.220	9.0	5240
10	**3**	−0.31	−0.10	0.210	8.2	3550

[a] $\Delta E = {}^2E_{1/2} - {}^1E_{1/2}$ in V vs Fc/Fc^+ set to 0.0 V. For the Fc/Fc^+ couple, $E° = 0.400$ V vs NHE.[54] [b] Metal−metal distances in Å in the transoid configuration. [c] The cobaltocenium analogue of polymer **1-100** with bromide anions.[55]

such a potential vs degree of oxidation profile, a linear chain of coupled redox centers will exhibit two waves in the cyclic voltammogram. In the region $0.1 < N < 0.45$ a large number of centers is oxidized for a relatively small change in the potential; that is, the "density of redox states", proportional to the inverse of the slope, is high. As the degree of oxidation nears 0.5, there is a rapid increase in $E°$ and a correspondingly low density of states in this region. The low density of states causes a decrease in the current vs voltage curve. As the degree of oxidation passes ca. 0.55, the potential levels off and there is again a high density of redox states and a second wave appears in the CV curve.

The separation of the two waves, ΔE, has been taken as a measure of the electronic interaction between the iron centers in the polymer backbone. The interaction may be expressed as a comproportionation constant (K_c) according to eq 1, where ΔE is in mV and $T = 298$ K.[34] A substance with $K_c = 0$ is classified as a class I material and exhibits no signs of electron transfer between mixed-valence sites. Values of K_c between zero and 10^5 indicate a class II material in which some electron transfer between mixed-valence sites occurs. A material with $K_c > 10^5$ is class III and exhibits complete electron delocalization at room temperature. However, the borderline between class II and class III systems is relatively soft and needs defining by more than one characterization method.

$$K_c = \exp(F\Delta E/RT) = \exp(\Delta E/25.69) \qquad (1)$$

The K_c's for **1** and **2** are 750 and 1630, respectively, as calculated from their ΔE's of 170 and 190 mV. These values are larger than that of diferrocenyl acetylene, $K_c = 160$, whose one-electron oxidized state is classified as a type II mixed-valence complex.[35] Values of the separation between the first and second waves for a variety of bi- and polyferrocenes are collected in Table 2. Also in Table 2 are the maximum Fe···Fe separations (estimates calculated with the assumption of fully transoid geometries) and the values of K_c as given by eq 1. The values of ΔE vs Fe···Fe distance (d_{Fe}) are plotted in Figure 3. Although there is an approximate inverse relationship between ΔE and d_{Fe} ($R = 0.74$), the main point to be gained from Figure 3 is that the points on the graph are *not* grouped into two sets: one set for conjugated spacers and one for nonconjugated. Thus, the Fe···Fe interactions (as measured by ΔE) for compounds

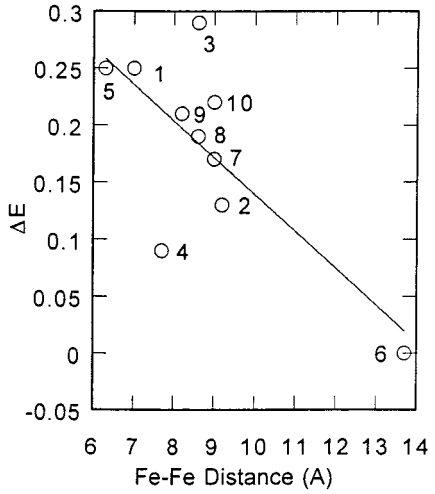

Figure 3. Plot of ΔE vs Fe−Fe distances. Numbers beside the data points correspond to the entry numbers of Table 2.

of the type Fc−(spacer)−Fc do not appear to be dependent on whether the spacer is conjugated. Instead, the Fe···Fe interactions would appear to be "through space". This conclusion is in accord with that recently derived by Lin et al. and by Deck et al.[19a,b] This is not to say that the bridging spacer has no effect on the Fe···Fe interaction. The "through space" interaction is mediated by the molecular-scale dielectric constant, i.e., on the polarizability of the intervening atoms. This idea finds some support in the data reported by Deck and coworkers, who found that fluorinated (less polarizable) spacers had lower ΔE's than the corresponding nonfluorinated spacers.[19b] The relative contributions of through space vs electronic delocalization through the spacer will depend on the degree of mixing between the frontier orbitals of the spacer and organometallic endgroups. Ferrocene ring-orbitals mix relatively weakly, so the Fe···Fe interactions are primarily through space. However, in compounds of the type $Cp(LL)Fe-(CC)_n-Fe(LL)Cp$, the ΔE's are larger for a given Fe···Fe distance, and the electron-transfer rates in the one-electron-oxidized compounds are rapid.[19c] In these compounds, Fe···Fe interaction appears to be spacer-mediated.

Relatively thick films of the polymers were deposited on the working CV-electrode by dipping the electrode in a polymer solution, removing the excess solution by shaking, and allowing the remaining solvent to evaporate. Cyclic voltammetry (acetonitrile containing 0.1 M Bu_4NPF_6 electrolyte) of the solid films does not show

(34) Hush, N. S. *Inorg. Chem.* **1967**, *8*, 391.
(35) Levanda, C.; Bechgaard, K.; Cowan, D. O. *J. Org. Chem.* **1976**, *41* (16), 2700.

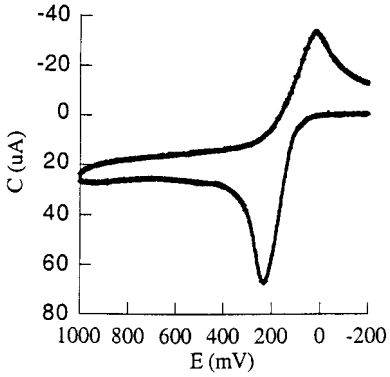

Figure 4. Cyclic voltammogram of **1** as a film on the Pt electrode (23 °C, 0.1 M NBu_4PF_6 electrolyte in CH_3CN solution at a scan rate of 200 mV/s).

the sharp, symmetrical reduction−oxidation peaks expected for an electrode-localized, electroactive film.[36] Instead, there is one unsymmetrical oxidation peak that occurs at 0.22 or 0.16 V for **1** or **2**, respectively. The neutral films are poorly solvated, highly resistive, and are not oxidized until a break-in potential (E_{bp}) is reached, at which point the electrolyte penetrates the film.[37] The oxidized films quickly dissolved from the electrode, as indicated by the discoloration of the electrolyte solution; hence, the return reduction current was always less than the oxidation current (Figure 4).

Oxidation of Polyferrocenes. When polymer **1** was oxidized with at least 1 equiv of elemental iodine, elemental analysis showed the presence of three I atoms per Fe atom. Magnetic measurements and IR spectra (see below) indicated that this material contained only Fe(III) centers. Hence, the stoichiometry of the oxidation of **1** with 1 equiv of I_2 is shown in eq 2. This polymer will be denoted as **1-100**. The numeral following the compound number is the degree of oxidation, *N*. The counterion is triiodide unless specified otherwise. Polymer **2-100** was synthesized by the oxidation of **2** with 1.5 equiv of I_2.

$$\mathbf{1} + 1.0\ I_2 \rightarrow (2/3)\ \mathbf{1\text{-}100} + (1/3)\ \mathbf{1} \qquad (2)$$

TGA's (heating rate of 40 °C/min, N_2 atmosphere) of **1-100** and **2-100** showed the occurrence of a 5% mass loss at 245 and 244 °C, respectively. The spectrum for **1-100** exhibited a plateau at 21% mass loss between 310 and 500 °C corresponding to the loss of one-half of the total iodine. The spectrum for **2-100** exhibited a plateau at 15% mass loss between 300 and 350 °C, corresponding to the loss of one-third of the total iodine. The partial loss of iodine from the oxidized polymers indicates some stability of the polymers with intermediate degrees of oxidation. Beyond their respective plateaus, both **1-100** and **2-100** showed a steady loss of mass up to 900 °C. The loss of iodine was confirmed by thermal degradation of the oxidized materials in a mass spectrometer. High-temperature decomposition (350 °C) of **1-100** in a mass spectrometer gave observed masses at 127 and 254 *m/z* (I^+ and I_2^+). The char yields of **1-100** and **2-100** at 900 °C were each ca. 30%.

(36) Peerce, P. J.; Bard, A. J. *J. Electroanal. Chem.* **1980**, *114*, 89.
(37) Nguyen, M. T.; Diaz, A. F.; Dement'ev, V. V.; Pannell, K. H. *Chem. Mater.* **1994**, *6*, 952.

Addition of I_2 to a CH_2Cl_2 solution of dimer **3** gave an immediate precipitate that analyzed as having excess iodine. This material is formulated as containing a mixture of undetermined polyiodides: **3-$(I_3)\cdot(I_2)_{2/3}$**

Partially Oxidized Polyferrocenes. The oxidation of **1** with 0.86 equiv of elemental iodine was expected to give a nominal degree of oxidation of 28% ("**I-28**") if triiodide were the only reduction product. However, the actual oxidation level was found to be 100% by comparison of the magnetic susceptibility data (vide infra) of **1-100** with that of "**I-28**". Rosenblum has reported that oxidation of similar polymers with a less than stoichiometric amount of iodine resulted in 100% oxidation of the iron centers and the formation of a mixture of iodide and triiodide counterions. Therefore, polymer **1** was completely oxidized with 0.86 equiv of I_2 according to eq 3 with the formation of 36% triiodide and 64% iodide anions.

$$\mathbf{1} + 0.86\ I_2 \rightarrow \mathbf{1}^+(I_3^-)_{0.36}(I^-)_{0.64} \qquad (3)$$
"**1-28**"

To prepare mixed-valence polymers, we investigated the comproportionation reactions of fully oxidized polymer with neutral polymer. In these mixed-valence polymers, the oxidation level, *N*, ideally corresponds to the moles of oxidized polymer divided by the total moles of oxidized and neutral polymer, $N = n/(n + y)$. Oxidized polymers **1-100** and **2-100** were dissolved in methylene chloride, one or more equivalents of the neutral polymer were added, and the solution was stirred at room temperature for 1 day. The solution was filtered and the solvent was removed. The residue was washed with hexanes to remove any neutral polymer, and the residue was dissolved again in methylene chloride. The mixed-valence polyionomer was precipitated by addition of hexanes. Interestingly, if more than 1 equiv of neutral polymer was allowed to react with the fully oxidized polymer, the hexane wash contained neutral polymer. Furthermore, the polyionomer could not be reduced below a level corresponding to ca. 55% oxidation despite the addition of more than 2 equiv of neutral polymer as described above.

The degree of oxidation of the mixed valence polyionomers was determined by carbon microanalysis. This determination assumes that the triiodide anion remained intact as the sole counterion during the Fc/Fc^+ electron-transfer reaction. The degrees of oxidation, as determined by this method, were supported by the Mössbauer data and UV−vis and IR spectroscopy (vide infra). As determined by the microanalytical method, mixed-valence polyionomers with the composition **1-55**, **1-62**, and **2-56** were formed from the equilibration reaction of fully oxidized polymer with the corresponding neutral polymer. The **1-62** composition was formed from the reaction of equimolar amounts of **1-100** and **1**. Hence, the course of the reaction may be written as eq 4. Note: eqs 4−6 are written as disproportionations of the "expected" composition for purposes of discussion only and do not imply the true mechanism (see below).

$$\mathbf{1\text{-}100} + \mathbf{1} \rightarrow 2\ [\mathbf{1\text{-}50}] \rightarrow 1.6\ \mathbf{1\text{-}62} + 0.39\ \mathbf{1} \qquad (4)$$

Polymer **1-55** was formed from the reaction of 1 equiv of **1-100** with 3 equiv of neutral **1** (the expected, nominal

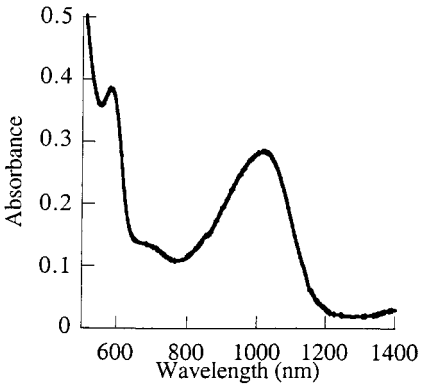

Figure 5. NIR absorption spectrum of $\mathbf{3}^{+}(\mathbf{I_3})\cdot(\mathbf{I_2})_{2/3}$.

product was **1-25**). Thus, eq 5 describes the formation of **1-55**.

$$\mathbf{1\text{-}100} + 3\ \mathbf{1} \rightarrow 4\ [\mathbf{1\text{-}25}] \rightarrow 1.88\ \mathbf{1\text{-}55} + 2.12\ \mathbf{1} \quad (5)$$

Similarly, polymer **2-56** was formed from the reaction of equimolar amounts of **2-100** and **2** according to eq 6.

$$\mathbf{2\text{-}100} + \mathbf{2} \rightarrow 2\ [\mathbf{2\text{-}50}] \rightarrow 1.78\ \mathbf{2\text{-}56} + 0.22\ \mathbf{2} \quad (6)$$

These curious results may be explained by reference to the Frost diagram, Figure 2. The slope of the line joining any two points in a Frost diagram is equal to the standard potential of the redox couple of the species that the two points represent. Hence, if some species **X** lies above a line connecting two species **Y** and **Z**, then **X** is unstable with respect to disproportionation into **Y** and **Z**. Conversely, **Y** and **Z** will comproportionate into **X** if the latter lies below the line connecting **Y** and **Z**. Hence, degrees of oxidation in region **A** and **C** (Figure 2) are stable with respect to disproportionation, whereas those in regions **B** and **D** are unstable. Hence, adding increments of neutral polymer to 100% oxidized polymer will initially cause some reduction, but any reduced level between ca. 0.85 and 1.0 (region **D**) will disproportionate to 85% and 100% oxidized material. Further addition of neutral polymer eventually reduces all the polymer to 85% oxidized, at which point reduction into region **C** occurs. These oxidation states are stable up to the limit of about $N = 50\%$. Further addition of reduced polymer does not result in mixed valence polymer with $0.15 < N < 0.50$, since these states in region **B** will disproportionate into almost fully reduced ($N = 0.15$) and 50% oxidized polymer. In actual practice, the disproportionation limits appear to be 55% and 0.0% oxidation levels since neutral polymer, not $N = 0.15$, is recovered from the reaction mixtures.

UV−Vis Spectroscopy. Band I of ferrocenium ion (617 nm in the parent ion, assigned to a ligand-to-metal charge transfer, $^2E_{2g} \rightarrow {}^2E_{1u}$) is useful in characterizing ferrocenium ions because of its relatively strong intensity and its separation from other absorptions. Band I was observed for the partial and the fully oxidized materials. Compounds **1-62**, **2-56**, and $\mathbf{3}\text{-}(\mathbf{I_3})\cdot(\mathbf{I_2})_{2/3}$ have transitions at 1015 nm ($\epsilon = 300\ M^{-1}\ cm^{-1}$), 1053 nm ($\epsilon = 470\ M^{-1}\ cm^{-1}$), and 1014 nm ($\epsilon = 1010\ M^{-1}\ cm^{-1}$), respectively (see Figure 5, for example). The fully oxidized polymers **1-100** and **2-100** have transitions at 1015 nm ($\epsilon = 500\ M^{-1}\ cm^{-1}$) and 1053 nm ($\epsilon = 890\ M^{-1}\ cm^{-1}$), respectively. A distinguishing feature of the absorption spectra is a long tail spanning the entire visual spectrum (Figure 6). The "tail" is responsible for the oxidized polymers appearing brown or black.

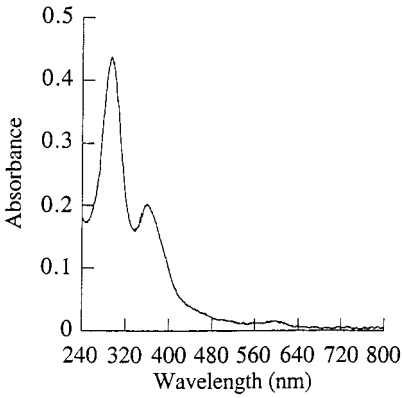

Figure 6. UV−vis absorption spectrum of $\mathbf{3}^{+}(\mathbf{I_3})\cdot(\mathbf{I_2})_{2/3}$.

Table 3. UV−Vis Data for Neutral and Oxidized Metallocene Materials[a]

compound	band II d^6 metal	band I d^5 metal	band II d^5 metal
1	460 (2000)		
2	468 (2800)		
3	455 (870)		
1-62		1015 (300)	
2-56		1053 (470)	
$\mathbf{3}^{+}(\mathbf{I_3})^{-}\cdot(\mathbf{I_2})_{2/3}$		1014 (1010)	582 (1370)
1-100		1015 (500)	
2-100		1053 (890)	

[a] The solvent was CH_2Cl_2 for all materials. λ_{max} in nm and ϵ in $M^{-1}\ cm^{-1}$.

Band II, assigned to the d−d transition, $^2E_{2g} \rightarrow {}^2E_{1g}$, is the second strongest of the ligand field transitions normally seen in ferrocenium salts.[27] With strongly electron-withdrawing groups attached to the Cp-ring, a π^* orbital may drop below the unoccupied d levels, so that this band acquires d−π^* character.[19d] In the parent Fc^+, band II is found at 565 nm, but the position is sensitive to substituent effects on the cyclopentadienyl ring system and may shift by 15 nm.[38] Of the materials prepared in this study, only $\mathbf{3}\text{-}(\mathbf{I_3})\cdot(\mathbf{I_2})_{2/3}$ exhibited a band II transition, at 582 nm ($\epsilon = 1370\ M^{-1}\ cm^{-1}$), as seen in Figure 5. Band II for the oxidized polymers was not observed. The lack of intensity may be due to the wide distribution of cyclic oligomers and long chain polymers, each possessing a different λ_{max}, which would spread the oscillator strength over a broad band and diminish its peak height.

Toma has investigated the effects of aryl substituents on band I of arylferrocenium salts.[30a] Since band I is an LMCT type of transition, its position depends greatly on the energy of the HOMO of the ligand. Thus, arylferrocenium salts with electron-donating groups substituted onto the aryl were observed to have a pronounced red shift from the parent compound, 1-phenylferrocenium. 1-Phenylferrocenium has a transition at 745 nm, while 4′-*N*,*N*-(dimethylamino)-1-phenylferrocenium exhibits a 1300 nm transition. The partially or fully oxidized Fc-polymers described here have transitions at ca. 1000 nm, indicative of a relatively

(38) Levanda, C.; Bechgaard, K.; Cowan, D. O. *J. Org. Chem.* **1976**, *41*, 2700.

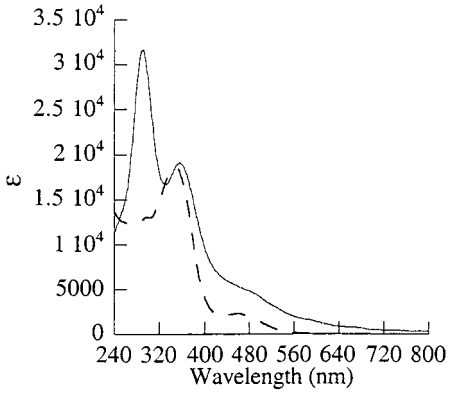

Figure 7. UV−vis absorption spectra of methylene chloride solutions of **1** (dashed line) and **1-100** (solid line).

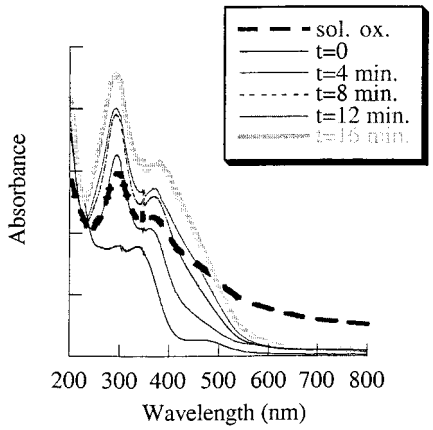

Figure 8. UV−vis absorption spectra of a 200 μm thick film of **1** oxidized with I_2 vapor for various times (solid lines) and of a film of **1-55** (dashed line) cast from solution.

high HOMO energy. Table 3 summarizes the UV−vis spectral data.

Figure 7 compares the UV−vis spectra of **1** and **1-100** in CH_2Cl_2 solution. In addition to the band II at 460 nm, **1** has a $\pi\rightarrow\pi^*$ transition at 348 nm and a barely discernible peak at 292 nm. Upon oxidation, the peak at 292 nm becomes much more intense, and the $\pi\rightarrow\pi^*$ transition shifts slightly to 356 nm while its intensity remains nearly constant. In the solid state, the $\pi\rightarrow\pi^*$ peak blue shifts to 334 nm and appears to decrease in intensity so that the 292 and 334 nm peaks have nearly the same height (t = 0 min, Figure 8).

Doped solid-state materials often exhibit electronic properties that are quite different from their solutions. Hence, the solid-state oxidation process was compared to oxidation in solution by monitoring the UV−vis spectra. Thin films of **1** and **2** (200 μm thick as measured by profilometry) were spin coated onto quartz disks from toluene solution (1 mg/mL). The films were exposed to iodine vapors in an enclosed chamber, removed from the development chamber every four minutes, subjected to a vacuum (0.5 Torr) to remove unreacted surface absorbed iodine, and weighed, and their spectra were taken before being placed back into the development chamber. The deposition rate of iodine was determined by placing a thick film of **1** of known surface area inside a closed chamber containing the solid iodine, allowing iodine vapor to react with the film, and recording the increase in mass over time. The deposition rate so determined was 25 mg/min·cm^2. The exposed films were observed to darken, and full oxidation, as shown by no further increase in weight, occurred after approximately 16 min of exposure. A 3:1 iodine-to-iron ratio was expected if triiodide were the counterion, but the iodine-to-iron ratio calculated from the weight gain was only 2:1 despite the large excess of iodine vapor available for reaction.

Figure 8 shows the effect on the spectra of films of **1** caused by oxidation with iodine vapor vs time. Also shown is the spectrum of a film of **1-55** deposited from a solution of the preoxidized polymer (**1-55**). The spectrum of the solution-oxidized material (**1-55**) is similar to that of the film-oxidized polymer, except for the tail extending across the visible region for the **1-55** film. The $\pi\rightarrow\pi^*$ peak, seen at 356 nm in solution, is red-shifted to 384 nm and becomes much more intense (Figure 8, t = 16 min). The peak at 292 nm also increases in intensity. The spectra of oxidized films dissolved in CH_2Cl_2 were identical to the spectra of **1** that had been oxidized by I_2 in solution.

The iodine-oxidized polymers are susceptible to de-doping both thermally or under high vacuum. Thin films of iodine-oxidized **1** and **2** were observed by UV−vis to thermally de-dope (100 °C, 1 atm) to neutral polymer in less than 1 h. Black **2-100** was observed to revert to its neutral red form, **2**, under high vacuum at room temperature in about 1 h. XPS of **2-100** and **2**, both stored at 10^{-9} Torr for 12 h, revealed identical iron signals at 708.5 eV, a value consistent with the literature value of neutral ferrocene.[39] Thus the iodine oxidation is reversible in the solid state (thermal or vacuum de-doping).

Electron Transfer. The mixed-valence polymers did not exhibit intervalent electron transfer (IT) bands. Near-IR (NIR) spectra of **1-62**, **2-56**, and **3-$(I_3)\cdot(I_2)_{2/3}$** exhibited no IT bands from 1200 to 2000 nm, where most IT bands involving ferrocenium dimers or polymers are usually found.[19d] Infrared spectroscopy has been employed also to study electron-transfer behavior in mixed-valence ferrocenes. Typically, neutral ferrocenes exhibit an absorption due to C−H out-of-plane bending from 805 to 825 cm^{-1} in the IR, whereas ferrocenium cations show the same vibration from 840 to 860 cm^{-1}. Molecular vibrations occur on the time scale of ca. 10^{-11} s. If the IR bands for a given mixed-valence material occur at a frequency intermediate between those for the corresponding neutral and fully oxidized species, then it can be concluded that the mixed-valence is delocalized on the IR time scale. Polymer **2** exhibited two bands associated with the C−H out-of-plane bend, a singlet at 829 cm^{-1} and another singlet at 839 cm^{-1}. The oxidized polymer **2-100** showed one band associated with the C−H out-of-plane bend at 874 cm^{-1}, consistent with the 100% oxidation level determined by microanalysis. The partially oxidized polymer **2-56** exhibited all the absorptions described above for **2** and **2-100**, but no peaks with intermediate frequencies were observed. Hence, **2-56** would not be considered a valence-delocalized system on the IR time scale. The C−H absorption bands for **1**, **1-55**, and **1-100** could not be resolved sufficiently to determine the extent of possible electron delocalization.

(39) Nguyen, M. T.; Diaz, A. F.; Dement'ev, V. V.; Pannell, K. H. *Chem. Mater.* **1994**, *6*, 952.

Chart 4

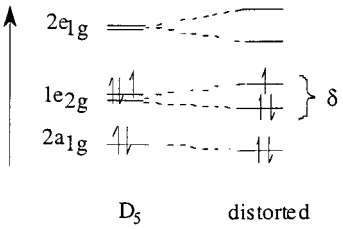

Chart 5

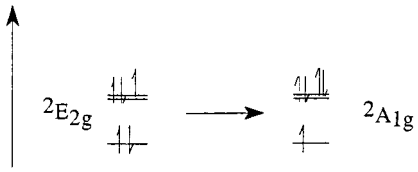

Table 4. Conductivity of Neutral and Oxidized Polymers

polymer	σ (S/cm)
1	$<10^{-10}$
1-55	$<10^{-10}$
1-100	9.0×10^{-9}
2	$<10^{-10}$
2-56	2.3×10^{-8}
2-100	6.5×10^{-7}

Conductivity of Films. The conductivity of **1**, **2**, and their respective partial and fully oxidized polymers was measured with a four-point probe. The results are collected in Table 4. The conductivity was calculated from eq 6:

$$\sigma = (I)(\ln 2)/(\pi t V) \qquad (6)$$

where t is film thickness in centimeters, I is the current in amperes, and V is applied voltage. Thick films of the materials were cast from tetrachloroethane, but only the neutral polymers formed good films. Films cast from solutions of the oxidized polymers were brittle, had many cracks, and had thicknesses that varied as much as 10 μm from an average of about 20 μm. Since an accurate conductivity measurement is dependent upon the uniformity of film thickness, an attempt was made at doping the better films formed from the neutral polymer by exposing them to iodine vapor. However, after long exposure to I_2, cracks were observed to form on the film's surface. Surface cracks result in barriers of infinite resistance and lower the measured conductivity considerably. Indeed, the measured conductivity of doped films did not increase using this approach. Inspection of Table 4 reveals the general trend that conductivity increased as percent oxidation increased. The conductivities are the same order of magnitude as those of other polyferrocenes reported in the literature; namely, the electrical conductivity of $[Fe(C_5H_4)_2SiMe_2]_n$-$(BF_4)_n$ is about 10^{-8} S/cm.[40]

Electron Paramagnetic Resonance. The EPR spectra of ferrocenium cations are only observable at very low temperature (<30 K). The d^5 $a_{1g}{}^2e_{2g}{}^3$ electronic configuration of ferrocenium cations results in a $^2E_{2g}$ ground state in D_5 symmetry, as seen in Chart 4. The

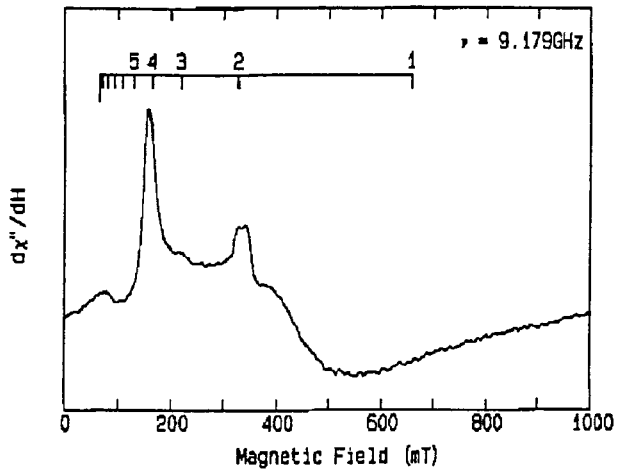

Figure 9. EPR spectrum of **1-55**.

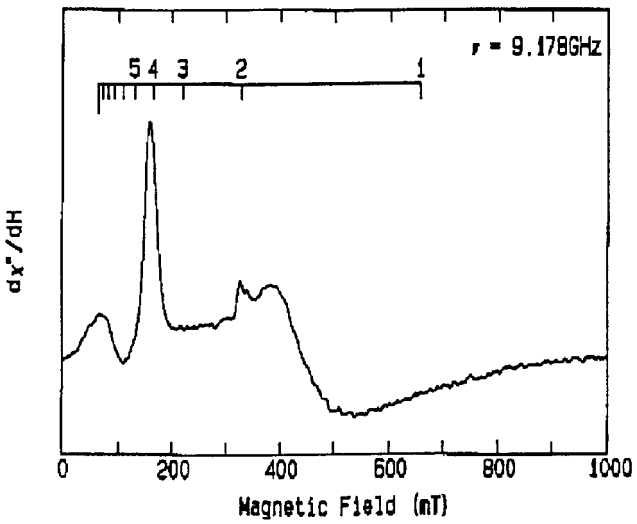

Figure 10. EPR spectrum of **1-100**.

^2E ground state allows for rapid spin−lattice relaxation and highly anisotropic g-tensors due to spin−orbit coupling. Prins has derived approximate g-value expressions appropriate for ferrocenium cations (eqs 7 and 8).[41]

$$g_z = g_{\parallel} = 2 + 4k[-(\xi/\delta)/(1 + \xi^2/\delta^2)^{1/2}] \qquad (7)$$

$$g_x = g_y = g_{\perp} = 2/(1 + \xi^2/\delta^2)^{1/2} \qquad (8)$$

In these equations, ξ is the spin−orbit coupling constant (ca. 328 cm^{-1} for Fe^{3+}),[42] k is the orbital reduction factor, and δ is a parameter that describes the splitting of the degeneracy of the e_{2g} orbitals; that is, δ is a measure of distortion from D_5 symmetry. The g-values for ferrocenium cations are generally very far from the free-electron g-value and are dominated by contributions from orbital angular momentum.

The EPR spectra of polymers **1-55** (Figure 9) and **1-100** (Figure 10) were measured on amorphous powder samples at 25 K. The measured g-values were identical for both samples: $g_{\perp} = 1.50$ and $g_{\parallel} = 4.27$. As is usual for ferrocenium ions, e.g., $[Fe(C_5H_5)_2]^+$ and $[Fe(Me_5C_5)_2]^+$, EPR spectra were not observed at 125 K.[43] In distorted ferrocenium ions with lowered symmetry and large

(40) Connor, J. A.; Derrick, L. M. R.; Hillier, I. H. *J. Chem. Soc., Faraday Trans. 2* **1973**, *69*, 941.

(41) Prins, R. *Mol. Phys.* **1970**, *19*, 602.

(42) Duggan, D. M.; Hendrickson, D. N. *Inorg. Chem.* **1975**, *14*, 995.

distortion parameters, δ, the g-tensor anisotropy, Δg, decreases and g approaches the spin-only value of 2.0. The g-anisotropy, $\Delta g = g_{\parallel} - g_{\perp}$, of 2.77 for both **1-100** and **1-55** is lower than for the parent ferrocenium ion (3.08) and reflects the lower symmetry of the Cp-ligand in the polymer repeat unit. However, the δ-values for **1-100** and **1-55** (372 cm^{-1}, calculated from eqs 7 and 8) are comparable to those of the ferrocenium (266 cm^{-1}), decamethylferrocenium (301 cm^{-1}), and octylmethylferrocenium ions (338 cm^{-1}).[44] This similarity suggests that splitting of the e_{2g} orbital caused by the asymmetric substitution pattern in **1-100** and **1-55** is not significant.

The effective magnetic moment at 25 K for both **1-100** and **1-55** was $\mu_{eff} = 2.38\ \mu_B$/ferrocenium center, as calculated by eq 9, where $\langle g \rangle$ is the mean g-value given by eq 10.

$$\mu_{eff} = \langle g \rangle [S(S+1)]^{1/2} \tag{9}$$

$$\langle g \rangle = [(g_{\parallel}^2 + 2g_{\perp}^2)/3]^{1/2} \tag{10}$$

It is significant that both **1-100** and **1-55** exhibit identical magnetic moments. Mixed-valence biferrocenes that either have delocalized electronic structures with no potential energy barrier for electron transfer or have an intramolecular electron-transfer rate faster than the EPR time scale have Δg values less than ~0.8. This is a reflection of considerably reduced orbital angular momentum in the delocalized ground state. Since the mixed-valence **1-55** and the fully oxidized **1-100** have identical magnetic moments, then the rate of electron transfer must be very slow. Thus the EPR results corroborate the conclusions based on the NIR and IR spectra.

Bulk Magnetic Behavior. The magnetic susceptibilities of the iodine-oxidized polymers have been measured. The samples, amorphous powders, were first cooled in a zero field, and the magnetic susceptibilities in a field of 0.1 T were determined in a SQUID magnetometer in the temperature range 5−300 K. For some of the oxidized polymers, e.g., **2-100** and **1-62**, the susceptibility data are well represented by Curie−Weiss behavior, $\chi = C/(T - \Theta)$, where $C = N\mu_{eff}^2/3k \approx \mu_{eff}^2/8$ (Figures 11 and 7S). For the phenylene polymers, plots of χ^{-1} vs T show a negative curvature over the entire temperature range, as shown in Figure 11 for **1-100** and in Figure 8S for **1-28**. This behavior has been observed previously for ferrocene polymers and oligomers and has been ascribed to the effects of large temperature-independent paramagnetism, to very large antiferromagnetic coupling between Fe sites, and even to long-range ferromagnetic interactions between Fe sites. We believe these explanations are erroneous and that the complex magnetic behavior is based on the complex magnetic behavior of ferrocenium ions themselves; that is, long-range magnetic ordering need not be invoked.

An alternate presentation of the data is shown in Figure 12 as a plot of χT vs T. At low temperature, χT of both **1-100** and **2-100** approach zero, characteristic of the weak antiferromagnetic interactions between

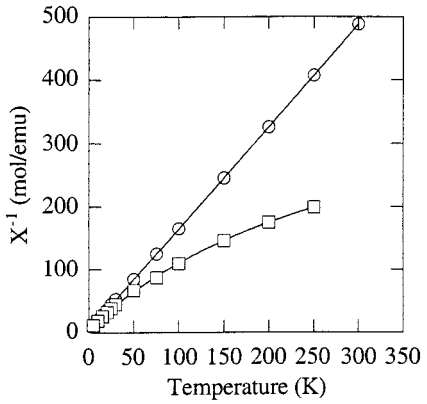

Figure 11. Plot of χ^{-1} vs T for **1-100** (□) and **2-100** (○).

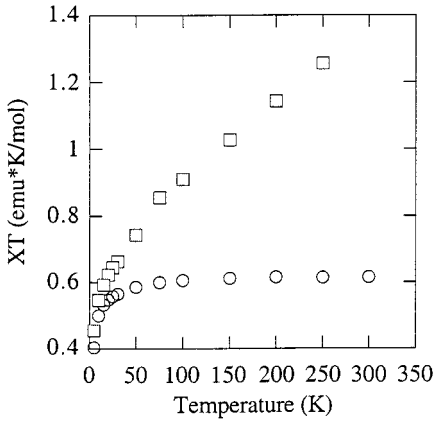

Figure 12. Plot of χT vs T for **1-100** (□) and **2-100** (○).

magnetic sites that gives rise to Curie−Weiss behavior. At higher temperatures, χT for **2-100** becomes constant as expected for normal Curie−Weiss paramagnets. However, χT for **1-100** becomes linearly proportional to the temperature. Hendrickson et al. showed some time ago that when the degeneracy of the $^2E_{2g}$ ground state of ferrocenium cation is lifted by low symmetry distortions, the magnetic moment may become temperature dependent.[21,45] The theoretical expression for the temperature dependency of χ is complex, but the functional form for the magnetic moment is quite simple: $\mu_{eff} = aT + b$. With this functional form, χT becomes linear in T at higher temperatures. Substitution of this functional form for μ_{eff} in the Curie−Weiss expression gives a good fit to the data with the values $\chi = (0.00341T + 2.36)^2/8(T + 3.2)$ for **1-100**, as shown by the solid line in Figure 11. Thus, at 300 K, $\mu_{eff} = 3.38\ \mu_B$ and $\Theta = -3.2$ K. The derived value for μ_{eff} at room temperature is slightly larger than those usually observed for ferrocenium ions at room temperature (2.3−2.6 μ_B).[21] However, the value of μ_{eff} at 25 K, calculated from the fitted expression $\mu_{eff} = 0.00341T + 2.36$, is 2.44 μ_B, in good agreement with the value based on the measured EPR parameters, 2.38 μ_B. Table 5 summarizes the magnetic susceptibility data for all oxidized materials. The materials are shown to exhibit weak antiferromagnetic coupling, as indicated by the small negative values of Θ.

Any ferrocenium ion with a distorted $^2E_{2g}$ state could have a temperature-dependent magnetic moment. How-

(43) (a) Warren, K. D. *Struct. Bonding (Berlin)* 1976, *45*, 45. (b) Prins, R. *Mol. Phys.* **1970**, *19*, 601.
(44) (a) Flandrois, D.; Chasseau, D. *Acta Crystallogr.* **1977**, *B33*, 2744. (b) Herbstein, F. H. *Perspect. Struct. Chem.* **1971**, *13*, 514.
(45) (a) Englemann, F. A. *Naturforsch. B* **1953**, *8*, 775. (b) Little, J. S.; Welcker, P. S.; Soy, N. J.; Todd, S. *J. Inorg. Chem.* **1970**, *9*, 63.

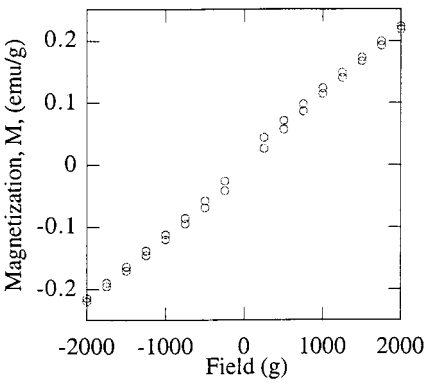

Figure 13. Field-dependent magnetization of the low-field region of **1-100** at 5 K.

Table 5. Magnetic Moments for Ferrocenium Compounds[a]

compound	μ_{eff} at 300 K	Θ_p, K	*a* (emu/mol) (slope)[b]	*b* (emu·K/mol) (intercept)[b]
1-100	3.38	−3.2	0.00341	2.36
1-85	3.40	−3.8	0.00316	2.45
1-55	2.91	−4.1		
2-100	2.24	−2.9		
2-56	2.77	−11.5		

[a] Diamagnetic corrections used: **1-100** -492×10^{-6} emu/mol; **1-85** -490×10^{-6}; **1-55** -702×10^{-6} emu/mol; **2-100** -479×10^{-6} emu/mol; **2-56** -682×10^{-6} emu/mol. [b] Variables *a* and *b* are defined as $\mu_{eff} = aT + b$ (see text).

ever, μ_{eff} for the majority of ferrocenium salts is found to be temperature independent. Hendrickson et al. have attributed the temperature independence of μ_{eff} to one of two possible causes: thermal population of a low lying electronic state, e.g., the $^2A_{1g}$ state (d,[5] $a_{1g}{}^1e_{2g}{}^4$ configuration), or a temperature-dependent, low symmetry distortion.[21] We have no explanation for why the thiophene-linked ferrocene polymers show normal Curie−Weiss behavior (temperature-independent μ_{eff}), but the phenylene-linked polymers have temperature-dependent moments.

Magnetization as a Function of an Applied External Field. Since there had been claims of ferromagnetic behavior in poly(ferrocenylene-*alt*-dimethylsilylene),[16] further magnetic characterization was obtained by analyzing the magnetization as a function of the applied external field. At 5 K the magnetization curve of **1-100** as a function of applied field exhibited a slight hysteresis (Figure 13), which may be indicative of ferromagnetic interactions. The observed coercive field was $H_c = 165$ G, and the remnant magnetization was $M_r = 162$ emu G/mol. However, saturation magnetization was not observed for **1-100** or **2-100** at 5 K nor for **1-100** at room temperature. Hence, the most likely explanation for the very small remnant magnetization is spin-glass formation. The spin-glass phenomenon results from a random distribution in the magnitude and sign of the interactions between neighboring moments in a magnetically dilute system. A net magnetic moment can arise from "frustration" of antiferromagnetically coupled spins in a random or amorphous lattice. A triangular lattice of antiferromagnetically coupled magnetic ions illustrates frustration, as portrayed in Figure 14 (adapted from Figure 3 of ref 46). If the nearest neighbor coupling constant, *J*, is negative, there is no arrangement of spins that simultaneously

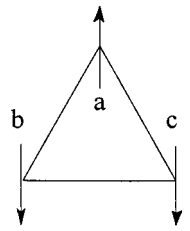

Figure 14. Illustration of spin-frustration in an antiferromagnetically coupled system of three spins.

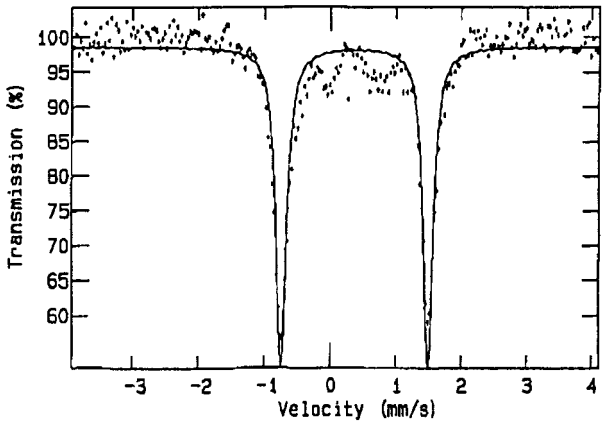

Figure 15. Transmission Mössbauer spectrum of **1**.

satisfies all the microscopic constraints: aligning any two spins antiferromagnetically means the remaining spin must be aligned with one of the other two. The system is thus frustrated.[46] At low temperatures, a net alignment of frustrated spins is "frozen" in, giving rise to magnetization curves that exhibit a small remnance magnetization, but not the saturation that is characteristic of ferromagnets; that is, the curve shown Figure 13 is typical.[47]

Mössbauer Spectroscopy. Mössbauer spectra were obtained on polymers **1**, **2**, **1-100**, and **1-55** at 125 K. As expected, the spectral parameters indicated that polymer **1** was entirely Fe^{II} in character, having one doublet with QS = 2.24 mm/s, and $\delta = 0.496$ mm/s (Figure 15).[48] The spectrum of polymer **2** was similar, having one doublet with QS = 2.25 mm/s and $\delta = 0.500$ mm/s. Unfortunately, neither **2-56** nor **2-100** exhibited a Mössbauer signal at 125 K, possibly because the samples had very low recoil-free fractions due to the soft matrix. The entirely oxidized polymer **1-100** exhibited a complicated set of interactions (Figure 16). The spectrum was resolved into three doublets with QS = 0.810, 0.377, and 0.190 mm/s and corresponding δ = 0.434, 0.491, and 0.575 mm/s, respectively, all assigned to Fe^{III} sites. The approximate ratio of the integrated areas beneath the doublets is 0.5:1.0:1.0. Presumably, the three types of doublets result from different Fe environments as a result of polymer conformations and counterion orientations.[49] The partially oxidized polymer **1-55** exhibited an even more complicated set of interactions: five doublets were observed with QS =

(46) Hurd, C. M. *Contemp. Phys.* **1982**, *23*, 469.
(47) Ford, P. J. *Contemp. Phys.* **1982**, *23*, 141.
(48) Feyerherm, R.; Litterst, F. J.; Burkhardt, V.; Nuyken, O. *Solid State Commun.* **1992**, *82* (3), 141.
(49) Dong, T.; Hendrickson, D. N.; Pierpont, C. G.; Moore, M. F. *J. Am. Chem. Soc.* **1986**, *108*, 963.

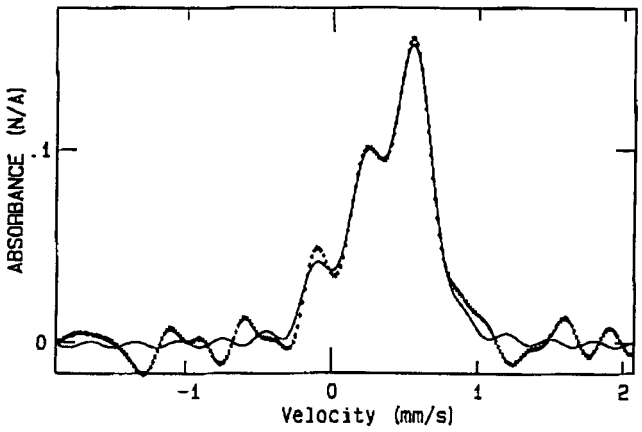

Figure 16. Absorbance Mössbauer spectrum of **1-100**.

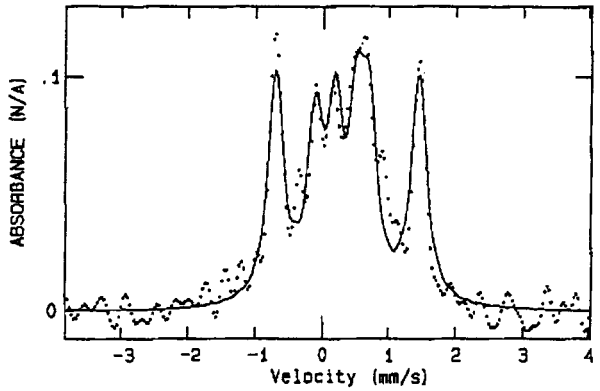

Figure 17. Absorbance Mössbauer spectrum of **1-55**.

2.15, 1.20, 0.810, 0.377, and 0.190 mm/s, with corresponding δ values of 0.494, 0.40, 0.434, 0.491, and 0.575 mm/s, respectively (Figure 17). The first doublet is assigned to localized Fe^{II} and the last three to localized Fe^{III}, and the second peak with QS = 1.20 is tentatively assigned to a delocalized mixed-valence $Fe^{2.5}$ site. Hence, at some sites in polymer **1-55**, electron transfer between Fe centers occurs faster than the Mössbauer time scale (ca. 10^7 s^{-1}), but not for other sites. The ratio of the integrated areas beneath the doublets assigned to Fe^{II} and Fe^{III} is 1.5:2:0. This ratio corresponds to 57% oxidation, which is in excellent agreement with the elemental analysis that indicates 56% oxidation. Attempts to obtain Mössbauer spectra at higher temperatures, where electron delocalization might be more pronounced, failed because no signal was detectable, most likely because of a drop in the number of recoil-free sites at higher temperatures.

Similar behavior has been observed previously,[50] and it is known that the Mössbauer spectra of biferrocenium monocations are greatly influenced by sample history. For example, samples of a biferrocenium salt exhibited two valence-localized doublets, one assigned to Fe^{III}, the other to Fe^{II}, as well as a doublet with $Q \approx 1.2$ that was assigned to valence-delocalized sites. The relative ratios of the intensities of these three doublets depended on temperature, the solvent used for crystallization, the rate of crystallization, and the counterion.[51]

Conclusions

New conjugated bis(cyclopentadienyl)arylene ligands 1,4-bis(3-hexyl-4-methyl-cyclopentadienyl)benzene and 2,5-bis(3-hexyl-4-methylcyclopentadienyl)thiophene have been synthesized. Upon treatment with FeI_2, these ligands formed soluble polymers based on the 3,3′-dihexyl-4,4′-dimethyl-1,1′-ferrocenylarylene repeat units in good yield. Significant amounts of cyclic oligomers are formed during the polymerization reaction. The neutral polymers form high-quality, amorphous films by spin-casting. Full oxidation of the polyferrocenes was possible with ≥1.0 equiv of iodine; however, controlled partial oxidation within the limits $0.5 < N < 1.0$ could only be accomplished by comproportionation between neutral and fully oxidized materials. As measured by CV, the polymers exhibited significant Fe···Fe interaction between ferrocene centers, but the mixed-valence polymers had little electron transfer between metal centers as measured by IR, NIR, and Mössbauer. The electrical conductivity of all the polymeric materials was very low: 10^{-10} to 10^{-8} S/cm. Some of the oxidized polymers exhibit unusual magnetic behavior with temperature-dependent magnetic moments, whereas others showed normal Curie−Weiss behavior. The unusual magnetic properties are ascribed to effects of the degenerate ground state of ferrocenium ions, not to any long-range magnetic ordering, as had been previously proposed.

Experimental Section

General Considerations. All reactions and manipulations were carried out under a nitrogen atmosphere using standard Schlenk line techniques or by use of an inert atmosphere glovebox. Dry solvents, when needed, were distilled from either Na/benzophenone (aromatics and ethers), CaH_2 (halogenated and nonhalogenated hydrocarbons), or CaO (nitrogen-containing solvents). Reagents were purchased from Aldrich Chemical Co., Lancaster, Janssen, or Strem Chemical, Inc. ^{1}H NMR data were collected on a Bruker AM-360, AM-300, or AM-200 spectrometer and were referenced to the residual proton solvent resonance. UV−vis spectra were collected on a Shimadzu 3101PC with baseline correction. Thermogravimetric analyses (TGA) were performed using a Perkin-Elmer apparatus. Cyclic voltammetry (CV) was performed with a C 214 poteniostat controlled by a PC running a program written by Dr. Steven Parus. FT-IR spectra were obtained on a Nicolet 5-DXB spectrometer. Mass spectra were collected on a VG 70-250-S high-resolution spectrometer. GC−MS data were collected on a Finnigan model 4500 spectrometer. Elemental analyses were performed by the Microanalysis Laboratory, Department of Chemistry, The University of Michigan, or Galbraith Laboratories, Knoxville, TN. Magnetic susceptibility measurements were taken on a Quantum Designs MPMS SQUID magnetometer with an applied field of 1000 G in the temperature range 10−300 K. Hystersis magnetization experiments were run at 5 or 300 K, and the applied fields were cycled from 10 000 to −10 000 G. The samples were contained in calibrated gelatin capsules held in the center of a soda straw fixed to the end of the sample rod. The magnetization values

(50) Mazur, U.; Hipps, K. W. *J. Phys. Chem.* **1982**, *86*, 2854.
(51) Dong, T.; Kambara, T.; Hendrickson, D. N. *J. Am. Chem. Soc.* **1986**, *108*, 4423.
(52) Nelson, J. M.; Nguyen, P.; Petersen, R.; Rengel H.; Macdonald P. M.; Lough, A. J.; Manners, I.; Raju, N. P.; Greedan, J. E.; Barlow, S.; O'Hare, D. *Chem. Eur. J.* **1997**, *4*, 573.
(53) Foucher, D. A.; Tang, B.; Manners, I. *J. Am. Chem. Soc.* **1992**, *114*, 6246.
(54) Koepp, H. M.; Wendt, H.; Strehlow, H. *Z. Elektrochem.* **1960**, *64*, 483.
(55) Southard, G. S.; Curtis, M. D. Unpublished work.

of the instrument were calibrated against a standard palladium sample supplied by Quantum Designs.

Solid-state UV−vis experiments were performed on polymer films that were spin coated onto quartz disks from toluene solution (1 mg/mL). Film thickness was measured by profilometry. For iodine doping experiments, an iodine development chamber was constructed of a covered glass slide dish approximately 3 in. in diameter with 10 g of crushed iodine placed inside the dish. The films were placed into the chamber, and the iodine deposition rate was determined from the mass increase vs time of a thick film of **1** of known surface. Before measuring the uptake of iodine, the exposed films were subjected to a vacuum (2 min, 0.5 Torr) to remove unreacted surface-absorbed iodine. A series of electronic spectra (Shimadzu 3101PC with baseline correction) of the films were obtained after 4 min intervals of I_2 exposures until no further change was recorded in the spectra. At this point, the weight gain corresponded to the uptake of two iodine atoms per Fe atom.

Hexylmethylcyclopent-2-en-1-one Isomers. Isopropyl 2-nonenoate (28.3 g, 143 mmol) was added dropwise over the course of 6 h to polyphosphoric acid (100 g) heated to 120 °C. The heating was continued for a further 6 h after the addition of the ester was complete. The reaction mixture was quenched with water (250 mL), and diethyl ether (200 mL) was added. The aqueous layer was removed, and the organic layer was washed with saturated aqueous sodium bicarbonate (2 × 50 mL) and dried over $MgSO_4$. The solvent was removed, and the product was distilled under vacuum (0.1 Torr, 80 °C) to give 8.8 g of yellow oil (34% yield based on isopropyl-2-nonenoate). Two isomers of the desired compound had been formed, 3-hexyl-4-methylcylopent-2-en-1-one (**A**) and 3-methyl-4-hexylcylopent-2-en-1-one (**B**). GC−MS, *m*/*z* (found/calcd; % area): 180 (180), 100%. ^{1}H NMR (300 MHz, 25 °C, C_6D_6): δ 5.81 (s, 1 H, vinylic C*H* of **A**); 5.76 (s, 1 H, vinylic C*H* of **B**); 3.20 (m, 1 H, C*H* of **A** and **B**); 2.80 (m, 1 H, C*H* of B); 2.61 (m, 2 H, CH_2 of **A** and **B**); 2.21 (m, 2 H, CH_2 of **A** and **B**); 1.85 (dd, 1 H, CH*H* of **A** and **B**); 1.80 (dd, 1 H, CH*H* of **A** and **B**); 1.49 (s, 3 H, CH_3 of **A**); 1.25 (m, 6 H, $(CH_2)_3$ of **A** and **B**); 0.96 (t, 3 H, CH_3 of **A** and **B**); 0.70 (d, 3 H, CH_3 of **A** and **B**). Anal. (found/calcd for $C_{12}H_{20}O$): C 80.64 (80.54); H 11.02 (11.18).

1,4-Bis(3-hexyl-4-methylcyclopentadienyl)benzene (mixture of isomers). A sample of 1,4-dibromobenzene (5.76 g, 24.4 mmol) was placed in a 250 mL Schlenk flask under N_2. Dry ether (50 mL) was added via cannula, and 2.5 M *n*-butyllithium (10.2 mL, 24.4 mmol) was added dropwise. After the solution was stirred for 20 min, a white precipitate formed. Hexylmethylcylopent-2-en-1-one (4.40 g, 24.4 mmol) was added dropwise, causing the precipitate to redissolve. The solution was heated to reflux for 1 h. More 2.5 M *n*-butyllithium (10.2 mL, 24.4 mmol) was added, causing a white precipitate to slowly form. The mixture was stirred for 1 h at room temperature, and additional hexylmethylcylopent-2-en-1-one (4.40 g, 24.4 mmol) was added dropwise, causing the precipitate to dissolve. After the solution was stirred for 1 h at room temperature and then heated to reflux for 30 min, it was cooled to room temperature and quenched with saturated aqueous NH_4Cl (2 × 100 mL). The aqueous phase was extracted with ether (2 × 30 mL), and the combined ether fractions were dried over $MgSO_4$. The solution was concentrated to about 30 mL, and *p*-toluenesulfonic acid monohydrate (700 mg) was added. After 10 min of stirring, a yellow precipitate was observed. The stirring was continued for 2 h, after which time sufficient ether was added to dissolve all of the precipitate. The ether solution was washed with water (3 × 100 mL) and dried over $MgSO_4$. The ether was removed to give the yellow solid product, which was recrystallized from hexanes to give 2.1 g (21% yield). ^{1}H NMR (300 MHz, 25 °C, C_6D_6): δ 7.47 (m, 4H, a); 6.81 (s, 1.2 H, b); 6.67 (s, 0.8 H, b′); 3.18 (s, 1.6 H, c′); 3.08 (s, 2.4 H, c); 2.31 (t, 4 H, d); 1.88 (s, 6 H, e); 1.56 (p, 4 H, f); 1.29 (bm, 12 H, g, h, and i); 0.91 (t, 6 H, j). Anal. (found/calcd for $C_{30}H_{42}$): C 89.10 (89.48); H 10.61 (10.51). Mass spectrum, *m*/*z* (found/calcd for $C_{30}H_{42}$): 402 (402).

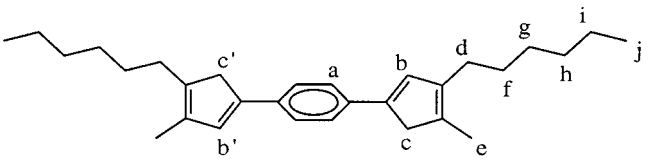

2,5-Bis(3-hexyl-4-methylcyclopentadienyl)thiophene (mixture of isomers). A sample of 2,5-dibromothiophene (5.35 g, 22.1 mmol) was placed in a 250 mL Schlenk flask under N_2. Dry ether (75 mL) was added via cannula, and 1.6 M *n*-butyllithium (19.4 mL, 31 mmol) was added dropwise. After the solution was stirred for 20 min, a white precipitate formed. Hexylmethylcylopent-2-en-1-one (4.00 g, 22.1 mmol) was added dropwise, causing the precipitate to redissolve. The solution was heated to reflux for 1 h. More 1.6 M *n*-butyllithium (19.4 mL, 31 mmol) was added, causing a white precipitate to slowly form. The mixture was stirred for 1 h at room temperature, and additional hexylmethylcylopent-2-en-1-one (4.00 g, 22.1 mmol) was added dropwise, causing the precipitate to dissolve. After the solution was stirred for 1 h at room temperature and then heated to reflux for 30 min, it was cooled to room temperature and quenched with saturated aqueous NH_4Cl (2 × 100 mL). The aqueous phase was extracted with ether (2 × 30 mL), and the combined ether fractions were dried over $MgSO_4$. The solution was concentrated to about 30 mL, and *p*-toluenesulfonic acid monohydrate (700 mg) was added. After 10 min of stirring the solution began to darken. The stirring was continued for 2 h. The ether solution was washed with water (3 × 100 mL) and dried over $MgSO_4$. The ether was removed to give a brown oil, which was purified via column chromatography on silica gel with hexane eluent to give a yellow oil upon removal of the hexanes (4.6 g, 52% yield). ^{1}H NMR (300 MHz, 25 °C, C_6D_6): δ 7.17 (m, 1 H, Cp*H*); 6.79 (m, 2 H, C4H_2S); 6.70 (dd, 1 H, Cp*H*); 3.08 (dd, 4 H, Cp CH_2); 2.19 (bm, 4 H, a-CH_2); 1.77 (bm, 3 H, CpCH_3); 1.44 (bm, 20 H, (CH_2)5); 0.89 (t, 6 H, $(CH_2)_5CH_3$). Anal. (found/calcd for $C_{28}H_{40}S$): C 81.90 (82.29); H 9.97 (9.87). Mass spectrum, *m*/*z* (found/calcd for $C_{28}H_{40}S$): 408 (408).

Poly(3,3′-dihexyl-4,4′-dimethyl-1,1′-diferrocenylene-*alt*-1,4-phenylene) 1, Method A. 1,4-Bis(3-hexyl-4-methylcylopentadienyl)benzene (1.5 g, 3.728 mmol) was dissolved in dry THF (30 mL) under N_2. Lithium diisopropylamide (0.885 g, 8.21 mmol) in THF (10 mL) was added via cannula. The dilithium salt of 1,4-bis(3-hexyl-4-methylcylopentadienyl)-benzene immediately precipitated. The yellow mixture was allowed to stir for 1 h before iron(II) iodide (1.154 g, 3.728 mmol) was added. The reaction mixture was heated to 50 °C for 5 days before being precipitated by pouring the mixture into methanol. The precipitate was collected, washed with MeOH, dried, redissolved in THF, and then reprecipitated by pouring the THF solution into a large excess of MeOH. The resulting precipitate was dried, and dissolved in chloroform, and the solution was filtered through Celite. Removal of solvent (Rotovap) gave a brittle red solid (1.2 g, 71% yield). ^{1}H NMR (300 MHz, 25 °C, C_6D_6): δ 7.46−7.36 (b, 3 H, C_6H_4); 6.79 (bs, 1 H, C_6H_4); 4.66 (bs, 0.6 H, Cp*H*); 4.60 (bs, 0.6 H, Cp*H*); 4.29 (bs, 2.8 H, Cp_H); 2.33−2.10 (bm, 4 H, α-CH_2); 1.86−1.73 (bm, 6 H, CpCH_3); 1.54 (bs, 4 H, β-CH_2); 1.32 (bs, 12 H, $(CH_2)_3$); 0.92 (bs, 6 H, CH_3). Anal. (found/calcd for ($C_{30}H_{40}Fe$)): C 79.06 (78.93); H 9.05 (8.83). FT-IR data (KBr, cm^{-1}): ν 3072 (CH aromatic stretch); 2955, 2926, 2844 (CH alkyl stretch); 1580 (CC aromatic stretch); 1466 (CC aromatic stretch); 833 (Cp CH out-of-plane bend).

Preparation of 1, Method B. 1,4-Bis(3-hexyl-4-methylcylopentadienyl)benzene (1.5 g, 3.728 mmol) was dissolved in dry THF (30 mL) under N_2. Lithium hexamethyldisilylamide (1.37 g, 8.21 mmol) in THF (10 mL) was added via cannula.

The dilithium salt of 1,4-bis(3-hexyl-4-methylcylopentadienyl)-benzene immediately precipitated. The yellow mixture was allowed to stir for 1 h before iron(II) iodide (1.154 g, 3.728 mmol) was added in increments of 100 mg/h. The reaction mixture was heated to 50 °C for 5 days before being worked up as described above. Removal of solvent (Rotovap) gave a brittle red solid (1.15 g, 68% yield). ^{1}H NMR (300 MHz, 25 °C, C_6D_6): δ 7.41 (b, 4 H, C6*H*$_4$); 6.95 (bd, 0.5 H, vinylic C*H*); 4.25 (bs, 4 H, Cp*H*); 2.28 (bs, 4 H, α-C*H*$_2$); 1.78 (bs, 6 H, CpC*H*$_3$); 1.50−1.32 (bs, 16 H, (C*H*$_2$)4); 0.92 (bs, 6 H, C*H*$_3$). Anal. (found/calcd for $(C_{30}H_{40}Fe)_{7n}(C_{30}H_{42})_n$): C 80.01 (80.11); H 9.15 (9.02). ^{13}C{^{1}H} NMR (90 MHz, 25 °C, C_6D_6): δ 136.0; 122.2; 89.5; 84.5; 83.9; 69.4; 68.4; 32.3; 31.4; 29.7; 27.7; 23.1; 14.4; 12.2. FT-IR data (KBr, cm^{-1}): ν 3072 (CH aromatic stretch); 2955, 2926, 2844 (CH alkyl stretch); 1580 (CC aromatic stretch); 1466 (CC aromatic stretch); 833 (Cp CH out-of-plane bend). UV−vis (λ_{max}, ϵ): 224 (15 770); 348 (16 440); 460 (2000). Gel permeation chromatography (chloroform, polystyrene standard, 1 mL/min, UV): M_n = 4000; M_w = 42 000; PDI = 10.5; DP = 9. Thermogravimetric analysis: 5% weight loss at 406 °C; 28% char yield at 900 °C.

Isolation of Dimer 3 (mixture of isomers). The dimer **3** was isolated by placing a sample of polymer **1** (method A) in a quartz tube, placing the tube in a tube furnace, and heating the sample to 390 °C under 0.01 Torr vacuum. The dimer (60 mg) was isolated from the wall of the quartz tube near the opening of the oven. ^{1}H NMR (300 MHz, 25 °C, C_6D_6): δ 6.97 (s, 8 H, C6*H*$_4$); 4.66 (bs, 4 H, Cp*H*); 4.61 (bs, 4 H, Cp*H*); 2.15 (bq, 8 H, α-C*H*$_2$); 1.77 (s, 6 H, CpC*H*$_3$); 1.73 (s, 6 H, CpC*H*$_3$); 1.40 (bm, 8 H, *β*-C*H*$_2$); 1.35 (bm, 24 H, (C*H*$_2$)3); 0.92 (bt, 12 H, C*H*$_3$). Anal. (found/calcd for $C_{60}H_{80}Fe_2$): C 78.58 (78.93); H 8.54 (8.83). Mass spectrum, *m/z* (found/calcd for $C_{60}H_{80}Fe_2$): 912 (912). UV−vis (λ_{max}, ϵ): 230 (19 320); 292 (18 260); 362 (6880); 455 (870). FT-IR data (PTFE, cm^{-1}): ν 3072, 3027 (aromatic CH stretch); 2953, 2925, 2854 (alkyl CH stretch); 827 (Cp CH out-of-plane bend).

Preparation of $3(I_3)\cdot(I_2)_{2/3}$ (undetermined polyiodide anions). Dimer **3** (60 mg, 0.066 mmol) was dissolved in a 1:1 hexane/benzene (15 mL) solution. Iodine (25 mg, 0.099 mmol) in a 1:1 hexane/benzene (15 mL) solution was added, causing the immediate precipitation of a brown solid. The brown solid was filtered, washed with hexanes, and dried (86% yield based on the formula as given and I_2 as the limiting reagent). Anal. (found/calcd for $C_{60}H_{80}Fe_2I_{4.33}$): C 49.10 (49.29); H 5.60 (5.52). UV−vis (λ_{max}, ϵ): 232 (32 400); 292 (86 590); 359 (38 520); 582 (1330); 1016 (980). FT-IR data (KBr, cm^{-1}): ν 3070, 3027 (aromatic CH stretch); 2953, 2925, 2854 (alkyl CH stretch); 837 (Cp CH out-of-plane bend).

Poly(3,3′-dihexyl-4,4′-dimethyl-1,1′-diferrocenylene-*alt*-2,5-thienylene) 2. 2,5-Bis(3-hexyl-4-methylcylopentadienyl)thiophene (3.022 g, 7.395 mmol) was dissolved in dry THF (30 mL) under N_2. Lithium hexamethyldisilylamide (2.72 g, 16.27 mmol) in THF (15 mL) was added via cannula. The dilithium salt of 2,5-bis(3-hexyl-4-methylcylopentadienyl)-thiophene remains soluble in THF. The dark brown mixture was allowed to stir for 1 h before iron(II) iodide (2.290 g, 7.395 mmol) was added in increments of 760 mg/6 h. The reaction mixture was heated to 50 °C for 5 days before the product was worked up as described for polymer **1**. Solvent removal gave a brittle red solid (1.6 g, 47% yield). ^{1}H NMR (300 MHz, 25 °C, C_6D_6): δ 6.84 (b, 2 H, C4*H*$_2$); 4.17 (bs, 4 H, Cp*H*); 2.25 (bs, 4 H, α-C*H*$_2$); 1.78 (bs, 6 H, CpC*H*$_3$); 1.50−1.30 (bs, 16 H, (C*H*$_2$)4); 0.91 (bs, 6 H, C*H*$_3$). Anal. (found/calcd for ($C_{28}H_{38}FeS$)): C 72.80 (72.71); H 8.24 (8.28). ^{13}C{^{1}H} NMR (90 MHz, 25 °C, C_6D_6): δ 130.0; 122.2; 89.5; 84.9; 80.5; 69.4; 68.4; 32.3; 31.4; 29.7; 27.7; 23.1; 14.4; 12.2. FT-IR data (KBr, cm^{-1}): ν 3070, 3029 (CH aromatic stretch); 2957, 2928, 2855 (CH alkyl stretch); 1458 (CC aromatic stretch); 1376 (CH alkyl bend); 829 (Cp CH out-of-plane bend); 686 (thienyl CH out-of-plane bend). UV−vis (λ_{max}, ϵ): 227 (14 560); 361 (14 240); 468 (2800). Gel permeation chromatography (chloroform, polystyrene standard, 1 mL/min, UV): M_n = 3600; M_w = 52 600; PDI = 14.6; DP = 8. TGA: 5% weight loss at 440 °C; 25% char yield at 900 °C.

Preparation of 1-100. Polymer **1** (100 mg, 0.33 mmol repeat unit) was placed into an 100 mL Schlenk flask, and iodine (84 mg, 0.33 mmol), dissolved in methylene chloride (10 mL), was added via cannula. The slurry immediately darkened to deep brown, and the mixture was allowed to stir for 18 h. The methylene chloride was removed, and the residue was washed with ether (2 × 50 mL) and redissolved in methylene chloride. The solution was filtered, and the product was precipitated by addition of hexanes. Filtration resulted in 100 mg (79% yield based on I_2 as the limiting reagent) of black polymer, **1-100**. Anal. (found/calcd for $[(C_{30}H_{40}Fe)_7(C_{30}H_{42})(I_3)_7]$): C 46.11 (46.02); H 5.08 (5.18) FT-IR data (KBr, cm^{-1}): ν 3065, 3030 (CH aromatic stretch); 2950, 2924, 2854 (CH alkyl stretch; 1471, 1453 (CC aromatic stretch); 840 (Cp CH out-of-plane bend); and 698 (CH aromatic bend). UV−vis (λ_{max}, ϵ): 219 (17 600); 289 (18 100); 356 (11 040).

Preparation of "1-28". Polymer **1** (100 mg, 0.22 mmol repeat unit) was placed into a 100 mL Schlenk flask, and iodine (48 mg, 0.19 mmol), dissolved in methylene chloride (10 mL), was added via cannula. The slurry immediately darkened to deep brown, and the mixture was allowed to stir for 18 h. The methylene chloride was removed, and the residue was washed with ether (2 × 50 mL) and redissolved in methylene chloride. The solution was filtered, and the product was precipitated by addition of hexanes. Filtration resulted in 84 mg (57% yield based on the stoichiometry of eq 3) of black polymer, **1-85**. Anal. (found/calcd for $[(C_{30}H_{40}Fe)_{7n}(C_{30}H_{42})_nI_{18n}]$): C 49.10 (49.16); H 5.52 (5.54). FT-IR data (KBr, cm^{-1}): ν 3065 (CH aromatic stretch); 2954, 2925, 2854 (CH alkyl stretch; 1600, 1471, 1453 (CC aromatic stretch); 837 (Cp CH out-of-plane bend); 698 (CH aromatic bend).

Preparation of 1-62. Fully oxidized polymer **1-100** (75 mg, 0.012 mmol repeat unit) and **1** (43 mg, 0.012 mmol repeat unit) were placed into a Schlenk flask containing methylene chloride (20 mL) under N_2 for 24 h. The black solution was filtered through Celite, the solvent was removed, and the residue was washed with ether (2 × 50 mL) and redissolved in methylene chloride. The solution was filtered, and the product was precipitated by addition of hexanes. A black powder was obtained (75 mg, 76% yield based on eq 4). Anal. (found/calcd for $[(C_{30}H_{40}Fe)_{7n}(C_{30}H_{42})_n(I_3)_{4.33n}]$): C 55.17 (54.90); H 6.27 (6.18). UV−vis (λ_{max}, ϵ): 220 (20 330); 290 (24 210); 351 (16 340).

Preparation of 1-55. Fully oxidized polymer **1-100** (50 mg, 0.008 mmol repeat unit) and **1** (86 mg, 0.024 mmol repeat unit) were placed into a Schlenk flask containing methylene chloride (20 mL) under N_2 for 24 h. The black solution was filtered through Celite, the solvent was removed, and the residue was washed with ether (2 × 50 mL) and redissolved in methylene chloride. The solution was filtered, and the product was precipitated by addition of hexanes. A black powder was obtained (80 mg, 105% yield based on eq 5). Anal. (found/calcd for $[(C_{30}H_{40}Fe)_{7n}(C_{30}H_{42})_n(I_3)_{3.85n}]$): C 57.09 (56.99); H 6.60 (6.41). FT-IR data (KBr, cm^{-1}): ν 3065, 3029 (CH aromatic stretch); 2953, 2927, 2855 (CH alkyl stretch); 1601, 1476, 1466 (CC aromatic stretch); 1377 (CH alkyl bend); 837 (Cp CH out-of-plane bend).

Preparation of 2-100. Polymer **2** (100 mg, 0.216 mmol repeat unit) was placed into a 100 mL Schlenk flask, and iodine (82.3 mg, 0.324 mmol), dissolved in methylene chloride (10 mL), was added via cannula. The slurry immediately darkened to deep brown, and the mixture was allowed to stir for 18 h. The methylene chloride was removed, and the residue was washed with ether (2 × 50 mL) and redissolved in methylene chloride. The solution was filtered, and the product was precipitated by addition of hexanes. Filtration resulted in 100 mg (55% yield) of black **2-100** being collected. Anal. (found/calcd for $[(C_{28}H_{38}FeS)(I_3)]$): C 40.14 (39.88); H 4.64

(4.54). UV−vis (λ_{max}, ϵ): 225 (14 210); 289 (27 100); 356 (18 130); 485 (6260). FT-IR data (KBr, cm^{-1}): ν 3065, 3029 (CH aromatic stretch); 2953, 2926, 2855 (CH alkyl stretch); 1451 (CC aromatic stretch); 1377 (CH alkyl bend); 840 (Cp CH out-of-plane bend); 698 (thienyl CH out-of-plane bend).

Preparation of 2-56. Fully oxidized polymer **2-100** (50 mg, 0.06 mmol repeat unit) and neutral polymer **2** (27 mg, 0.06 mmol repeat unit) were placed into a Schlenk flask containing methylene chloride (20 mL) under N_2 for 24 h. The black solution was filtered through Celite, the solvent was removed, and the residue was washed with ether (2 × 50 mL) and redissolved in methylene chloride. The solution was filtered, and the product was precipitated by addition of hexanes. A black powder was obtained (50 mg, 70% yield based on the stoichiometry of eq 6). Anal. (found/calcd for $[(C_{28}H_{38}FeS)_n(I_3)_{0.56n}]$): C 49.45 (49.77); H 5.59 (5.67). FT-IR data (KBr, cm^{-1}): ν 3065, 3029 (CH aromatic stretch); 2953, 2926, 2855 (CH alkyl stretch); 1451 (CC aromatic stretch); 1377 (CH alkyl bend); 840 (Cp CH out-of-plane bend); 698 (thienyl CH out-of-plane bend). UV−vis (λ_{max}, ϵ): 220 (16 300); 289 (24 860); 356 (18 181); 485 (5830).

Acknowledgment. We thank the donors of the Petroleum Research Fund, administered by the American Chemical Society, for support of this research. Special thanks go to Dr. W. R. Dunham for obtaining the Mossbauer spectra, and to Prof. M. Banaszak-Holl for obtaining XPS spectra.

Supporting Information Available: Graphs of CV curves and magnetic susceptibility vs temperature curves. This material is available free of charge via the Internet at http://pubs.acs.org.

OM000722Z